IDO-16543
Progress Reports
TID-4500 (14th Edition)

MTR-ETR TECHNICAL BRANCHES QUARTERLY REPORT
Period Ending March 31, 1959

August 19, 1959

AEC RESEARCH AND DEVELOPMENT REPORT

PHILLIPS PETROLEUM CO.
ATOMIC ENERGY DIVISION
(UNDER CONTRACT NO. AT (10-1)-205)
IDAHO OPERATIONS OFFICE
U. S. ATOMIC ENERGY COMMISSION

DISCLAIMER

PRICE $2.00

Available from the
Office of Technical Services
U. S. Department of Commerce
Washington 25, D. C.

LEGAL NOTICE

MTR-ETR TECHNICAL BRANCHES QUARTERLY REPORT
Period Ending March 31, 1959

PHILLIPS PETROLEUM COMPANY
Atomic Energy Division
MTR-ETR Technical Branches

J. R. Huffman	Assistant Manager, Technical
D. R. deBoisblanc	Director, Reactor Physics and Engineering
J. E. Evans	Director, Nuclear Physics
W. B. Lewis	Director, Theoretical Physics and Applied Mathematics

The Materials Testing Reactor, Engineering Test Reactor, and associated research and development facilities are operated by
Phillips Petroleum Company
Atomic Energy Division
under Contract AT(10-1)-205 to
Idaho Operations Office
U. S. Atomic Energy Commission

Previous Quarterly Reports in the MTR-ETR Series

1957

Quarter	Number
1	IDO-16373
2	IDO-16394
3	IDO-16430
4	IDO-16436

1958

Quarter	Number
1	IDO-16471
2	IDO-16481
3	IDO-16505
4	IDO-16534

MTR-ETR TECHNICAL BRANCHES QUARTERLY REPORT
First Quarter 1959

TABLE OF CONTENTS

		Page
I.	SUMMARY	1
II.	MTR TECHNICAL ASSISTANCE	3
	A. Linearization of MTR Burnup Curves for Estimation of Charge Life and Comparison of Charges	3
	B. Relative Statistical Weights in the MTR	5
	C. Shim Rod Drive Speed Increase	7
III.	ETR TECHNICAL ASSISTANCE	13
	A. Statistical Weight Measurements	13
	B. Control Rod Effects on Neutron Flux	13
	C. Cycle 13 Loading Mockup	15
IV.	REACTOR PHYSICS AND ENGINEERING	17
	A. Radiation Effects on Materials	17
	B. Metal-Water Reactions Program	17
	C. Fuel Element Development	19
	1. Sample Fuel Plate Irradiation Program	19
	2. Hydraulic Tests on Experimental MTR Shim Rod	20
	3. Lifetime Measurements on Cadmium Sections	21
	4. GCPR Fuel Element Development	21
	D. Thorium Program	22
	E. Reactor Physics Constants	22
	F. An Automatic Counting System for Gold Foils	25
	G. A Gamma Insensitive Control System for RMF-Type Reactors	26
V.	NUCLEAR PHYSICS	29
	A. Cross Sections Program	29
	1. Thermal Eta Measurement for U-233	29
	2. Fast Chopper Total Cross Section Measurements	29
	3. Fast Chopper Improvements	31
	4. Cross Section IBM-650 Programs	31
	5. Fast Chopper Energy Scale	31
	6. Monochromating Crystal Studies	32
	B. Nuclear Chemistry	33
	1. Mass Yields as a Function of Neutron Energy	33
	2. Calculation of the Composition of Pile-Irradiated Th-232, U-233, U-235, U-238 and Pu-239	34
	3. Studies of Niobium-94	35
	4. U-235 Alpha Experiment	38
	5. Pile Neutron Capture Cross Section of Co-60	39
	C. Inelastic Scattering of Slow Neutrons Program	40
	1. Inelastic Scattering Data for Steam, Methane and Vanadium	40

TABLE OF CONTENTS

		Page
	2. Preliminary Measurements on Graphite, Water, Nickel and Beryllium	48
	3. Mechanical Modifications of Velocity Selector	48
	4. Electronic Modifications of Velocity Selector	49
D.	Decay Scheme Studies	50
	1. The Decay of 23 min Sm-155	50
	2. Absolute Beta-Ray Counting Using a 4 π Windowless Flow Proportional Counter	56
VI.	THEORETICAL PHYSICS	60
A.	A Two Dimensional Study of ETR Fluxes and Burnout with the IBM-704 Program "TURBO"	60
B.	Calculations on the Scattering of Slow Neutrons by Free Water Molecules	63
C.	Applied Mathematics	69
	1. Heat Conduction Equation	69
	2. Fourier Analysis of Periodic Wave Forms	70
	3. Numerical Inversion of Laplace Transforms	70
VII.	PAPERS AND PUBLICATIONS	71
A.	AEC Report Issued	71
B.	Paper presented at the New York American Physical Society Meeting	71
C.	Journal Publications	71

LIST OF FIGURES

Figure No.	Title	Page
II-1	Idealized burnup curve obtained from MTR Cycles 81-113	4
II-2	Transformation for the MTR shim rod position to obtain a linear burnup curve	4
II-3	Transformed burnup curves of 10 MTR charges plotted on a special linearizing coordinate system	5
II-4	Available charge life in the MTR as determined from linearization of burnup curves as a function of average shim rod position at 60 Mwd of operation	6
II-5	Relative statistical weights in the MTR	8
II-6	Comparison of power excursions in the MTR for three cases calculated to approximate startup accidents	11
II-7	Comparison of the rates of power reduction from two speeds of reverse and a Junior Scram	12
III-1	The vertical distribution of statistical weights for U-235 and boron in the ETRC with data normalized to average values at 1.0	14

LIST OF FIGURES

Figure No.	Title	Page
III-2	Percentage change in thermal neutron flux when Control Rods No. 10 and No. 13 are withdrawn	15
III-3	Comparisons of ETR Cycle 6 and Cycle 13 horizontal midplane thermal neutron flux distributions	16
IV-1	Iron whisker bent to an elastic bending strain of 1.5% (Mag. 23X)	18
IV-2	Simplified version of proposed control system for RMF-type reactors used in the analog computer study.	27
V-1	Decay Scheme of Niobium-94 (energies in Mev)	38
V-2	MTR Neutron Velocity Selector	41
V-3	The scattering of 0.0446 ev neutrons from methane	42
V-4	The scattering of 0.0267 ev neutrons from methane	42
V-5	The scattering of 0.017 ev neutrons from methane	43
V-6	The scattering of 0.063 ev neutrons from methane	43
V-7	The scattering of 0.088 ev neutrons from methane	44
V-8	The scattering of 0.132 ev neutrons from methane	44
V-9	The scattering of 0.515 ev neutrons from methane	45
V-10	The scattering of 0.0267 ev neutrons from steam	45
V-11	The scattering of 0.0446 ev neutrons from steam	46
V-12	The scattering of 0.063 ev neutrons from steam	46
V-13	The scattering of 0.088 ev neutrons from steam	47
V-14	The scattering of 0.137 ev neutrons from steam	47
V-15	25 min Sm-155	52
V-16	Coincidence gamma-ray spectrum showing radiation in coincidence with 0.142 Mev gamma-ray	53
V-17	Coincidence gamma-ray spectrum showing radiation in coincidence with 0.106 Mev gamma-ray	54
V-18	Proposed level scheme for decay of 23 min Sm-155	55
V-19	Proportional counter discrimination curve using A-8 amplifier (weak Cs-137 source)	58
V-20	Highvoltage characteristics of 4 π proportional counter	59
VI-1	Two-dimensional spatial composition description of the ETR core	61
VI-2a	Upper Left Quadrant. Thermal flux history at the center of each 3 in.-square section of the core	64
VI-2b	Upper Right Quadrant. Thermal flux history at the center of each 3 in.-square section of the core	65
VI-2c	Lower Left Quadrant. Thermal flux history at the center of each 3 in.-square section of the core	66
VI-2d	Lower Right Quadrant. Thermal flux history at the center of each 3 in.-square section of the core	67

LIST OF TABLES

Table No.	Title	Page
II-1	Calculated Startup Accident	10
IV-1	Rates of Weight Gain for Selected Metals and Alloys upon Oxidation at Elevated Temperatures	19
IV-2	Data and Results for Special Thorium Slug	23
IV-3	Comparison of Calculated and Experimental Reactivities in the RMF	24
V-1	Cross Sections and Decay Constants Used for Heavy Element Calculations	36
V-2	Calculations of the Composition of Irradiated Th-232.	37
V-3	Co-60 Production as a Function of Φt	40
V-4	Energies and Intensities of Sm-155 Gamma-Rays	55
VI-1	Initial Description of the 23 Compositions	62
VI-2	Fraction of Total Power Generated in Each Composition for Each Time-Step	68

MTR-ETR TECHNICAL BRANCHES QUARTERLY REPORT
Period Ending March 31, 1959

I. SUMMARY

The more significant results and accomplishments in the technical program at the Materials Testing Reactor - Engineering Test Reactor during the first quarter of 1959 are summarized below.

In reactor technical assistance, a linearization technique was developed which yields a good prediction of charge life for MTR after a core has operated for some 60 Mwd. A detailed comparison of (1) relative statistical weights proportional to the square of neutron flux, and (2) experimental statistical weights, showed the two in good agreement, both for MTR and for ETR. An MTR startup accident calculation (void formation neglected) indicated that doubling the withdrawal rate for shim rods increases the calculated energy release in the power transient by only 3%. In an investigation of service life of MTR shim rods, examination of a Be-Cd rod that had logged 20,000 Mwd revealed that the Cd had changed to flakes; a fuel-Cd rod with 2545 Mwd of service showed no corrosion damage.

RMF measurements of the build-up of U-233 in MTR-irradiated Th slugs, made as part of a continuing program, were analyzed and results are presented. A gamma-insensitive control system for RMF-type reactors has been proposed, based on a loop through which a liquid circulates from the reactor core to an external detector where its neutron activation is measured. A stability study showed flow control requirements to be reasonable.

Additional total cross sections were measured with the crystal spectrometer and fast chopper, including those for Pu-240, U-235, U-233, Au, V, C, and B (in the thermal region) and for Pa-231, Np-237, and Ir (in the energy region < 10 ev). Energy calibration for the fast chopper has been improved by certain recalibrations and corrections. A study of competing planes in crystals disclosed that competition between planes may cause serious discrepancies in crystal spectrometer measurements of reactor spectra. In the inelastic scattering studies, steam, methane, and vanadium measurements were completed and preliminary measurements were made on graphite, water, nickel, and beryllium. Results are shown. A set of curved slits installed in the rotors has improved resolution of the velocity selector system.

The relative ratios of asymmetric to symmetric fission in Pu-239 for thermal and 0.29 ev neutrons were measured. The compositions of pile-irradiated Th-232, U-233, U-235, U-238, and Pu-239 were calculated from latest cross section values for different pile neutron spectra. A decay scheme was found for Nb-94 and Nb-94m.

A new energy level scheme for Eu-155 was developed from measurements of gamma-rays emitted from a neutron-irradiated sample of Sm-154. Preliminary studies of operational characteristics of a 4π counting system indicated that reliable precision determinations of absolute beta disintegration rates are readily obtained.

A succession of IBM-704 runs with the TURBO code was found to give a good picture of ETR flux changes during the course of an operating cycle.

The code furnishes a powerful tool for handling the problems of an unsymmetrical core. In addition to giving eigenvalues and flux distributions, which are obtainable from the simpler PDQ code, TURBO gives burnup of "burnable" nuclides for any specified time interval.

Two important codes were developed for the IBM-650. One gives a solution to the problem of heat flow from a spatially distributed source during transient conditions, which has direct application to pressure vessels such as are used in in-pile loops and SPERT. The other is a code for inversion of Laplace Transforms by numerical methods, of value in studies of reactor control systems, where it often is necessary to perform this operation.

II. MTR TECHNICAL ASSISTANCE

A. Linearization of MTR Burnup Curves for Estimation of Charge Life and Comparison of Charges (A. W. Brown, R. S. Marsden, J. M. Day, D. W. Miller)

To aid in evaluating the operation of the MTR on special fuels the characteristics of the change in reactivity with megawatt-days of operation have been examined closely. In addition to a direct comparison of the curves for the special fuels against that for normal fuel, a method has been developed which predicts the charge life of a loading for the early part of the cycle. This allows interpretation of charge data not otherwise available from a special fuel loading which might not last the full cycle.

The analyses of curves of shim rod position versus megawatt-days of operation for MTR Cycles 81A through 113B indicate that there is a marked similarity of the curves after 50 to 60 Mwd of operation with xenon equilibrium. Since many of these loadings were not burned out completely the curves were adjusted so that the resulting values of megawatt-days between shim rod positions of 25 and 30 in. are identical, then a translation was made which resulted in all curves going through the value of 600 Mwd at 30 in.

Result of this adjusting and translating procedure is two common points for the burnup curves, with some scatter of points at translated shim rod positions less than 25 in. By averaging the points at given shim rod positions an "idealized" burnup curve was obtained for shim rod motion between 25 and 30 in. The idealized curve was then extrapolated back to a shim rod position of 19 in. by use of a number of loadings which were not completely burned out but which had low values of the initial shim rod position. The portions of these burnup curves which corresponded to the idealized curve already obtained were fitted to the idealized curve and more points of the idealized curve were then obtained by averaging points at lower shim rod positions. The final idealized burnup curve is given in Fig. II-1. This curve may be used to obtain a transformation of the shim rod position which yields a straight line when plotted against megawatt-days of operation. The transformation curve which will convert the idealized burnup curve given in Fig. II-1 to a straight line is shown in Fig. II-2.

The available charge life of loads with incomplete burnup can then be approximated by determining from the curve shown in Fig. II-2 the transformed shim rod position and plotting the transformed position versus actual megawatt-days of operation, then extrapolating the resulting line to a shim rod position of 30 in. To facilitate this extrapolation, special coordinate paper was made with a non-linear scale, determined by the transformation given in Fig. II-2, for the shim rod position. Examples of the use of such coordinate paper are shown in Fig. II-3. Plotted on the figure are burnup curves of several charges which were operated until the shim rods were withdrawn to 30 in. Fig. II-3 demonstrates that the burnup curves are indeed similar in shape, as originally postulated. It is to be noted that this transformation straightened the burnup curves not only for the usual highly-enriched uranium loadings for the MTR, but for the 20%-enriched uranium and the plutonium loadings as well. Since this transformation yields a straight line for all three types of core, the shape of the burnup curve

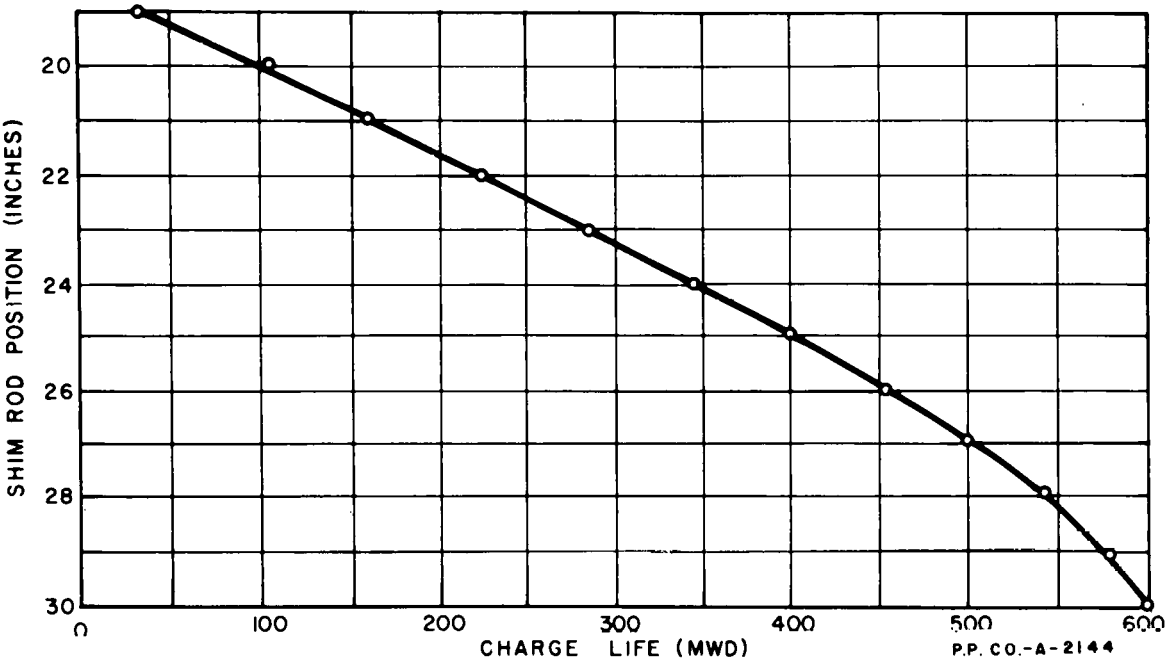

Fig. II-1 Idealized burnup curve obtained from MTR Cycles 81-113.

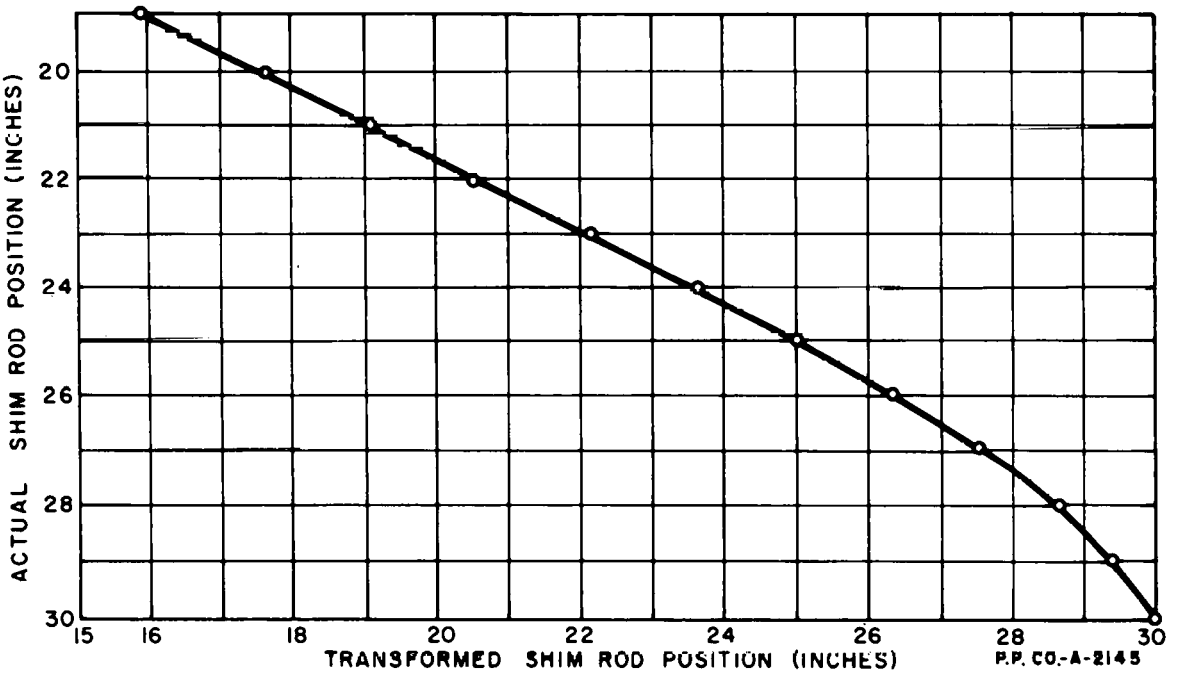

Fig. II-2 Transformation for the MTR shim rod position to obtain a linear burnup curve.

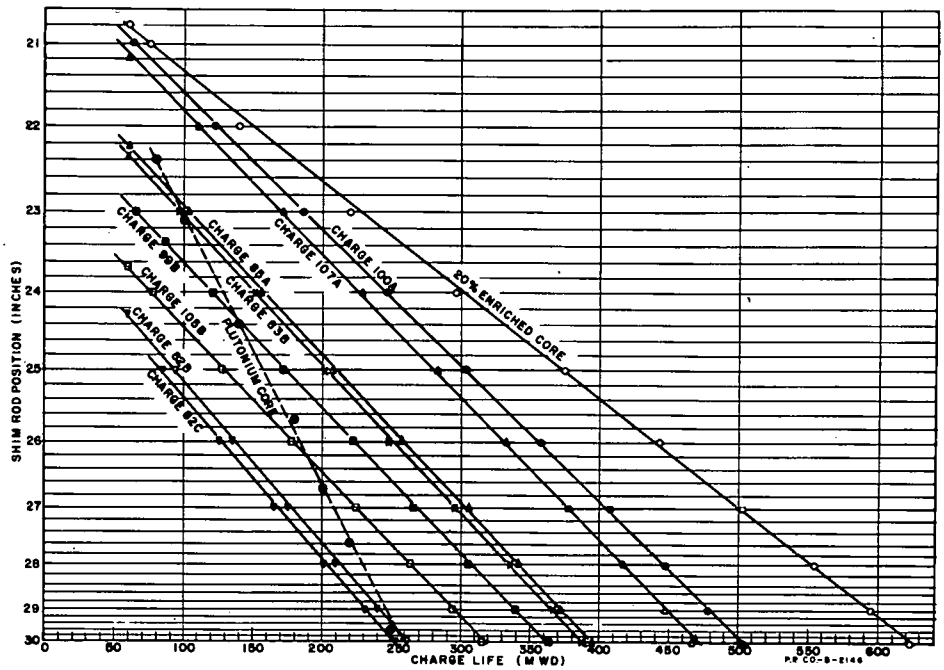

Fig. II-3 Transformed burnup curves of 10 MTR charges plotted on a special linearizing coordinate system.

must be almost entirely dependent upon the geometry of the reactor and independent of the fuel that is used, and there are no large non-linear effects from the formation of higher isotopes which add either poison or fissionable isotopes during the burnup of the cores of special fuel.

By use of the coordinate paper of Fig. II-3, the available charge life of each of a number of charges between reactor cycles 81A and 113B were found, then plotted versus the position of the shim rods when the reactor had been operated just 60 Mwd. This plot is given in Fig. II-4. From this plot it is possible to obtain a rough estimate of the life of a charge after just 60 Mwd of operation and of the life of charges whose operations were interrupted after only slightly more than 60 Mwd.

B. Relative Statistical Weights in the MTR (A. W. Brown, R. S. Marsden, J. M. Day, D. W. Miller)

It has been shown to be possible to make reliable estimates of relative statistical weights for MTR core positions by use of perturbation theory and neutron flux measurements made with cobalt wires. This approach is especially valuable for use in computing weights for cores where, in the absence of full data, neutron flux values are the only available basis for the computation.

According to one-group perturbation theory for an unreflected reactor or a very large reactor, the effect on reactivity of inserting fuel or absorber is proportional to the square of the thermal neutron flux at the point of

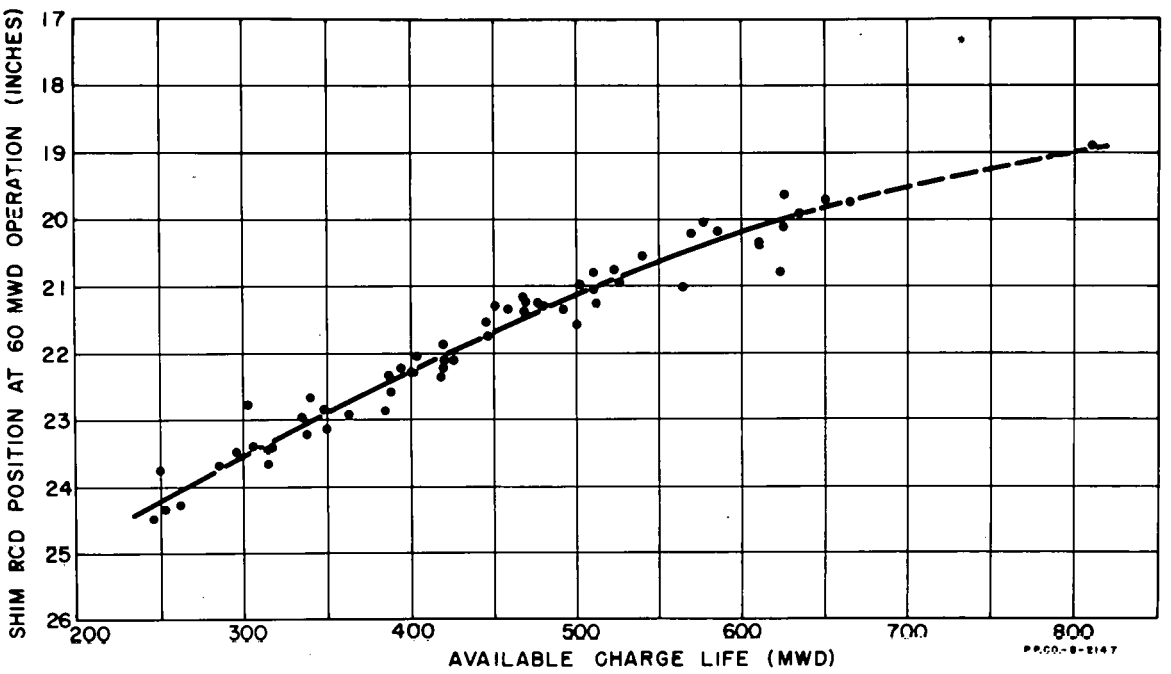

Fig. II-4 Available charge life in the MTR as determined from linearization of burnup curves as a function of average shim rod position at 60 Mwd of operation.

insertion. There have been a number of MTR loads where the neutron flux was monitored by means of cobalt wires inserted in each element. This method of measuring the neutron flux results in a curve of neutron flux versus vertical position for each fuel element. By squaring each value of flux on these curves and finding the integral of the square of the flux over the fuel length in each fuel element, it is possible to estimate relative statistical weights for each core position.

In addition to the many neutron flux measurements that have been made in the MTR core there have been three cores for which the poison relative statistical weights have been measured in a number of lattice positions, and one core for which fuel relative statistical weights have been measured. During the second loading of the MTR, poison statistical weights were measured in a number of positions after completion of the reactivity calibration of the shim rods with distributed poison.* To make the statistical weight measurements the poison was removed from one of the elements and the element moved from position to position with the critical shim rod readings being noted for each core position measured. Thus the measured weights were for a shim rod position of about 30 in. (rods pulled out to the maximum). After the first core had been burned up, a flux monitor wire was placed in each fuel element. The wires were then irradiated after the fission product poisons had decayed sufficiently to allow the reactor to become critical with the shim rods at 30 in. The measured statistical weight values and the integral of the square of the measured flux values

---

* deBoisblanc, Nyer, and Huffman, "Start-up of the Materials Testing Reactor", IDO-16028 (1953).

over each fuel element are given in Fig. II-5(a). These values have been normalized so that lattice position 25 has a weight of 1.00. Relative statistical weight measurements were made on the unpoisoned core of the MTR loaded with 20%-enriched uranium* and with the reactor loaded with plutonium.** These measurements were made by moving an element containing poison from position to position within the core. With the plutonium core, fuel statistical weight measurements were made using a special fuel element containing less fuel than the other elements. The neutron flux in each fuel element of the clean cold core was also measured in both of these special cores. The measured statistical weights and the integral of the square of the measured flux values over each fuel element from these two special loads are given in Fig. II-5(b) and II-5(c). These values have also been normalized so that lattice position 25 has a weight of 1.00.

The agreement for the three cores between the measured weights and those computed from the measured neutron flux is quite good, considering that the values of neutron flux for each element are probably not the best because of difficulty in correctly positioning the flux monitor wire in each element. However, the agreement obtained shows that good values of relative statistical weights can be computed, by use of the one-group perturbation approximation, for MTR cores in which only neutron flux values are available.

C. Shim Rod Drive Speed Increase (K. V. Moore, W. J. Byron)

The speed of the shim rod drive is a critical factor in determining whether the MTR can recover from a scram before xenon buildup causes it to stay shut down. This is because the magnets must be lowered to recouple them to their rods before the reactor can be returned to full power operation.

In the MTR's original design, drive speed was deliberately set slow to provide safe withdrawal speed for the rods. Recently it was decided to study modifications of the drive system that would make possible rapid insertion but would prevent accidental rapid withdrawal. As previously reported,*** tests made with one shim rod drive motor rewired to permit double-speed rod insertion indicate that two minutes can be cut from scram recovery time.

Although blocks were included in the proposed system to preclude double-rate rod withdrawal, a study of the consequences of accidental rapid withdrawal has been made. An investigation into the nature of the transient power overshoot that would occur for an accidental double-speed withdrawal revealed that the overshoot is higher, but occurs in about half the time as the one that occurs under normal speed conditions. Most important is that the integrated power resulting from the double speed withdrawal is

---

* D. R. deBoisblanc and R. S. Marsden, "Preliminary Evaluation of the 20%-Enriched Uranium Core for the Materials Testing Reactor", IDO-16459 (1958).

** D. R. deBoisblanc and R. S. Marsden, "Operation of the MTR on a Plutonium Loading", IDO-16508 (1958).

*** Moore, Petree, Byron, "MTR-ETR Quarterly Report for Period Ending December 31, 1958, IDO-16532, 2 (1959).

(a) 93 % ENRICHED URANIUM CORE

	1	2	3	4	5	6	7	8	9
1	0.357 0.37 —	0.552 — —	0.771 — —	0.836 — —	0.897 0.80 —	0.757 — —	0.688 — —	0.485 — —	0.260 — —
2	0.410 — —	— — —	0.820 — —	— — —	1.000 1.00 —	— — —	0.668 0.75 —	— — —	0.223 0.30 —
3	0.408 0.51 —	0.598 — —	0.864 0.83	1.013 — —	1.027 0.96 —	0.918 0.91 —	0.682 0.81 —	0.505 0.57 —	0.295 0.32 —

(b) 20 % ENRICHED URANIUM CORE

	1	2	3	4	5	6	7	8	9
1	0.246 0.21 —	0.390 — —	0.671 — —	0.778 — —	0.797 0.85 —	0.772 — —	0.537 0.58 —	0.361 0.35 —	0.173 0.19 —
2	0.287 — —	— — —	0.764 — —	— — —	1.000 1.00 —	— — —	0.631 0.67 —	— — —	0.164 0.17 —
3	0.307 0.27 —	0.539 — —	0.815 — —	0.960 — —	0.970 1.06 —	0.867 — —	0.664 — —	0.535 — —	0.184 0.19 —

(c) PLUTONIUM CORE

	1	2	3	4	5	6	7	8	9
1	0.240 0.22 —	0.350 — —	0.666 0.63 —	0.713 — —	0.973 0.92 0.84	0.841 — —	0.705 — —	0.507 0.50 —	0.326 — —
2	0.243 — —	— — —	0.692 — —	— — —	1.000 1.000 1.000	— — —	0.824 0.83 0.80	— — —	0.309 0.33 —
3	0.256 0.27 —	0.411 — —	0.715 0.641 —	— — —	1.042 1.28 1.09	1.211 — —	0.895 0.98 0.86	0.732 — —	0.374 0.45 0.40

XXX — COMPUTED FROM NEUTRON FLUX MEASUREMENTS
YYY — MEASURED VALUES FOR POISON
ZZZ — MEASURED VALUES FOR FUEL

P.P.CO.-A-2148

Fig. II-5 Relative statistical weights in the MTR.

only 3% higher than is the case with normal speed. These calculations do not consider the effect of void formation and thus are intended to be pessimistic. They also utilize experimentally established values of shim rod drop performance and control systems characteristics.

For the investigation the space-independent reactor equations were solved numerically for both the startup accident and the shutdown reactor power decay with the following conditions:

1. Startup accident power excursion for

   (a) regular speed continuous withdrawal of all shim rods, with reactor power level scramming one rod with an effective reactivity of δk_T = 10%,

   (b) double speed continuous withdrawal of all shim rods, scramming as in (a),

   (c) double speed continuous withdrawal of all shim rods where a period scram occurs for a reactor period less than 0.5 sec, with δk_T = 10%.

2. Shutdown reactor power decay for

   (a) regular speed continuous insertion of all shim rods ("Reverse"), with δk_T = 40%,

   (b) double speed continuous insertion of all shim rods as in 2(a), and

   (c) dropping one Be shim rod ("Junior Scram") with an acceleration downward of a = 3g, with δk_T = 3%.

In the case of the period scram, 1(c), the period reaches 0.5 sec before the Log N safety channel is in the operating range. It was arbitrarily chosen to activate this safety channel at 40 w as a reasonable time for which response would be available. Some of the pertinent data used and results obtained in (1), above, are summarized in Table II-1.

The transient power curves shown in Fig. II-6 were integrated for the total energy release. The suprising result is that doubling the withdrawal speed only increases the total energy yield from 12.2 to 12.6 Mw-sec. Curves of shutdown reactor power decay appear in Fig. II-7.

The results of these calculations were used by the Operations Engineering Branch for analysis of the power transient effect on heat transfer. The conclusion is that the double-speed withdrawal rate is permissible if only the fuel in the core is considered. When a similar series of calculations is made for the fuel-bearing experiments, if there is the same small difference in energy yield, it seems appropriate that the shim rod motors be changed to double-speed operation in both directions.

Table II-1

CALCULATED STARTUP ACCIDENT

	Case 1(a)	Case 1(b)	Case 1(c)
Shim Rods			
No. rods withdrawn*	All	All	All
Withdrawal rate, in./min	4.5	9	9
No. rods scrammed**	One	One	One
Scram acceleration, g	-3	-3	-0.7
Magnet release time τ, sec	0.015	0.015	0.015
Power Levels, Mw			
N_o	4×10^{-6}	4×10^{-6}	4×10^{-6}
N_1 (scram iniation)	60	60	4×10^{-5}*
N_{max} (peak power)	89.1	120.2	4.54×10^{-5}
Energy Yield, Mw-sec			
E	12.2	12.6	3.24×10^{-5}

* δk_T = 10%

** δk_T = 10%

* 1/2 sec period

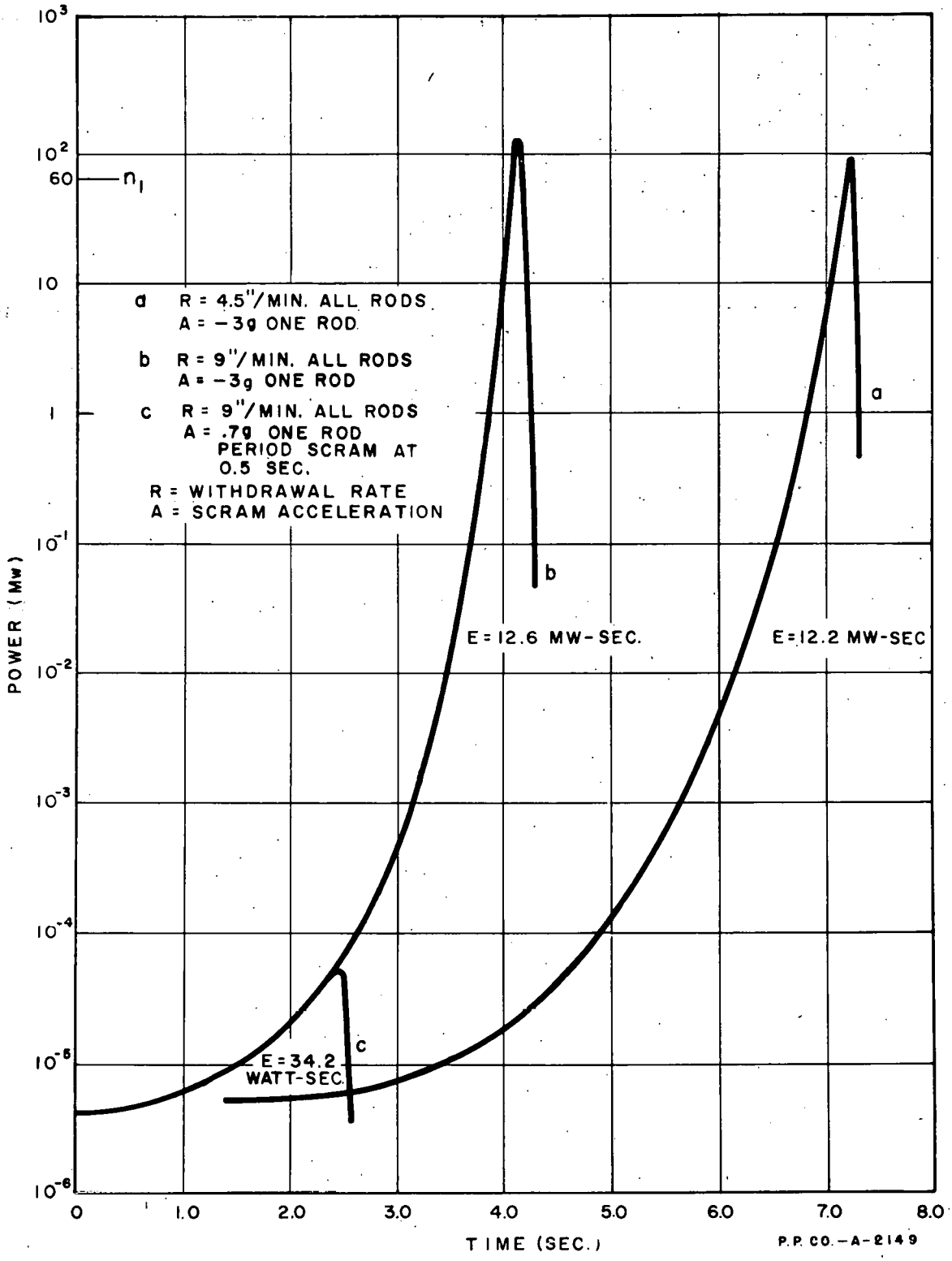

Fig. II-6 Comparison of power excursions in the MTR for three cases calculated to approximate startup accidents.

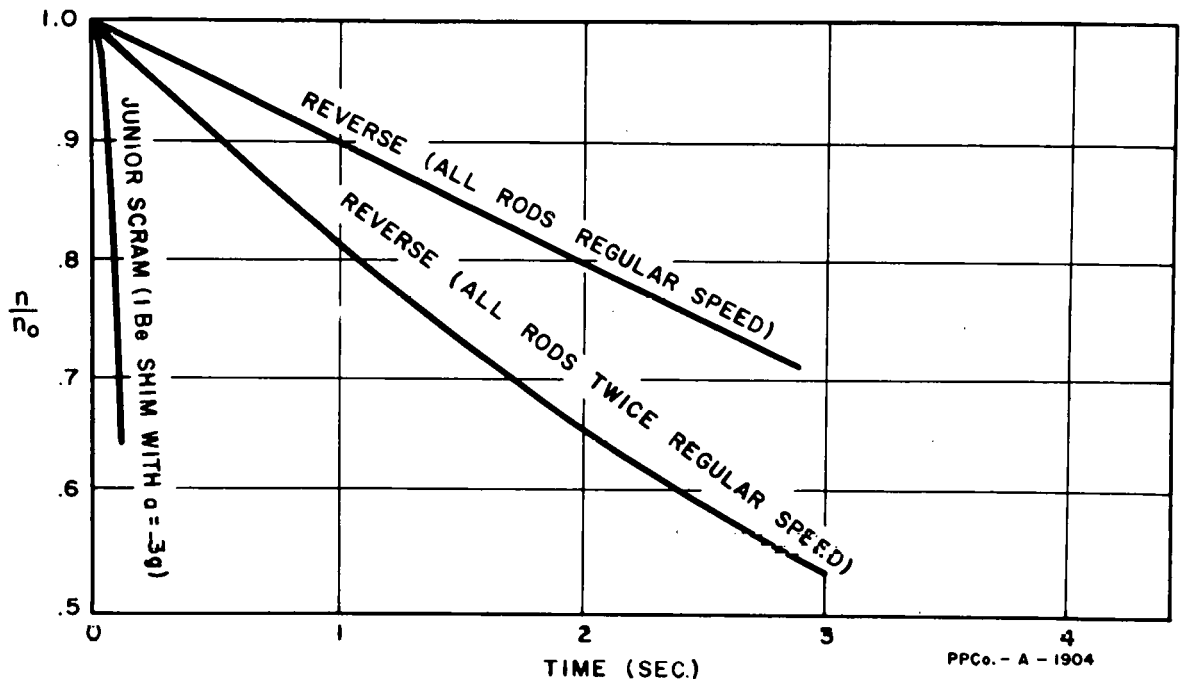

Fig. II-7 Comparison of the rates of power reduction from two speeds of reverse and a Junior Scram.

III. ETR TECHNICAL ASSISTANCE

A. Statistical Weight Measurements (J. W. Henscheid)

The statistical weight* of boron as a function of distance above the core midplane has been determined experimentally in the ETR Critical Facility. The measurements were made by moving stepwise a lateral distribution of 3 in.-sections of boron-impregnated polyethylene tapes (0.4 gm natural boron total) vertically through the water channels of a fuel element. The results of this experiment are shown in Fig. III-1. Also plotted in this figure are the results of a similar experiment with U-235** and a calculated curve proportional to the square of the measured thermal flux. Both the experimental data and the flux squared curve are normalized such that their average is unity, to permit their comparison.

The error limits on the data shown in the figure are the standard deviation of reactivity determinations in the ETRC. In general, the correlation between the statistical weight data and the flux squared curve is quite good. Up to 16 in. above midplane, the flux squared curve is within 18% of the experimental points.

An immediate application of the experimental data is in the determination of the reactivity effects of burnup (both U-235 and boron) in the ETR, which in turn can be used to obtain the excess reactivity in mixed loadings of used and new ETR fuel elements. Since burnup in a fuel element is a function of the flux distribution in that element, the average statistical weight (as measured in a cold, clean core) will not yield accurate values for the associated reactivity effects. However, if the assumption is valid that the statistical weight distribution as well as the burnup distribution can be obtained from a flux measurement, the resulting changes in reactivity should be easily and more accurately calculated.

B. Control Rod Effects on Neutron Flux (E. E. Burdick, D. L. Parry, R. M. Eckert***)

The highest heat flux does not occur at the start of a cycle in the ETR with the present sequence for withdrawing the gray rods. At present, Rods No. 10 and 13 are withdrawn individually and in that order; then No. 6, 8, 11, and 16 are withdrawn simultaneously. No. 10 and No. 13, being at the center of the core tend to increase the central neutron flux as they are withdrawn, while No. 6, 8, 11, and 16, being around the outside of the core, tend to increase the peripheral neutron flux and consequently decrease the central neutron flux. Since criticality usually occurs at about 18 in. on Rod No. 10, the highest heat flux will probably occur during withdrawal of No. 13.

---

* Defined here as the reactivity per unit weight of the sample.

** E. E. Burdick, "MTR-ETR Branches Quarterly Report Period Ending December 31, 1958", IDO-16532, 7, (1959).

*** Visiting engineer from Public Service Electric and Gas Company of New Jersey.

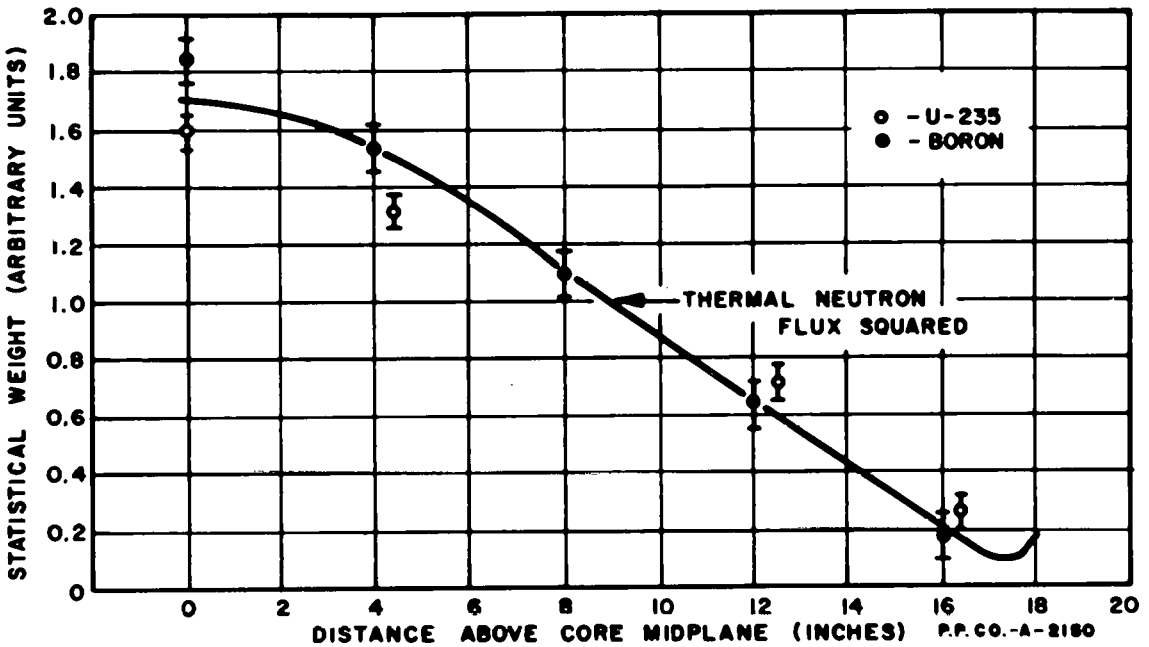

Fig. III-1 The vertical distribution of statistical weights for U-235 and boron in the ETRC with data normalized to average values at 1.0.

Three neutron flux runs were made in the ETRC to measure the changes in the neutron flux during the withdrawal of these rods. The measurements were made near the center of each element with gold foils placed on lucite strips. The rod positions for the three runs were: Rod No. 10 at 18 in., Rod No. 10 at 36 in. (upper limit), and Rod No. 13 at 36 in. In the second and third cases the core was uniformly poisoned with boron-impregnated polyethylene tapes to simulate xenon poisoning and to permit withdrawal of No. 10 and 13. The poison was adjusted so that the position of the driven Shim Rod No. 7 very nearly reproduced its position in the first run. The effects of withdrawing these rods are presented in Fig. III-2 as the percentage change in the neutron flux for each fuel position in the core. Not shown in the figure, but of significance, is the fact that the "hot spot" was adjacent to Rod No. 10, that it remained there throughout these measurements, and that the hot spot flux increased by 10%.

The correspondence of flux behavior between the ETRC and ETR for the first part of an ETR cycle is quite good. The buildup of xenon in the ETR causes both Rods No. 10 and 13 to reach their upper limits in less than twenty hours after startup; therefore, there is negligible effect on neutron distributions due to burnup. With the ETR operating at 175 Mw (full power), the minimum thermal neutron flux is greater than 10^{14} n/cm^2-sec except at the very corners of the core. Since the xenon concentration has very little dependence on flux above fluxes of 10^{14} n/cm^2-sec, the concentration is almost uniform throughout the core. These conditions are essentially duplicated in the uniformly distributed poison of the experiment as described above.

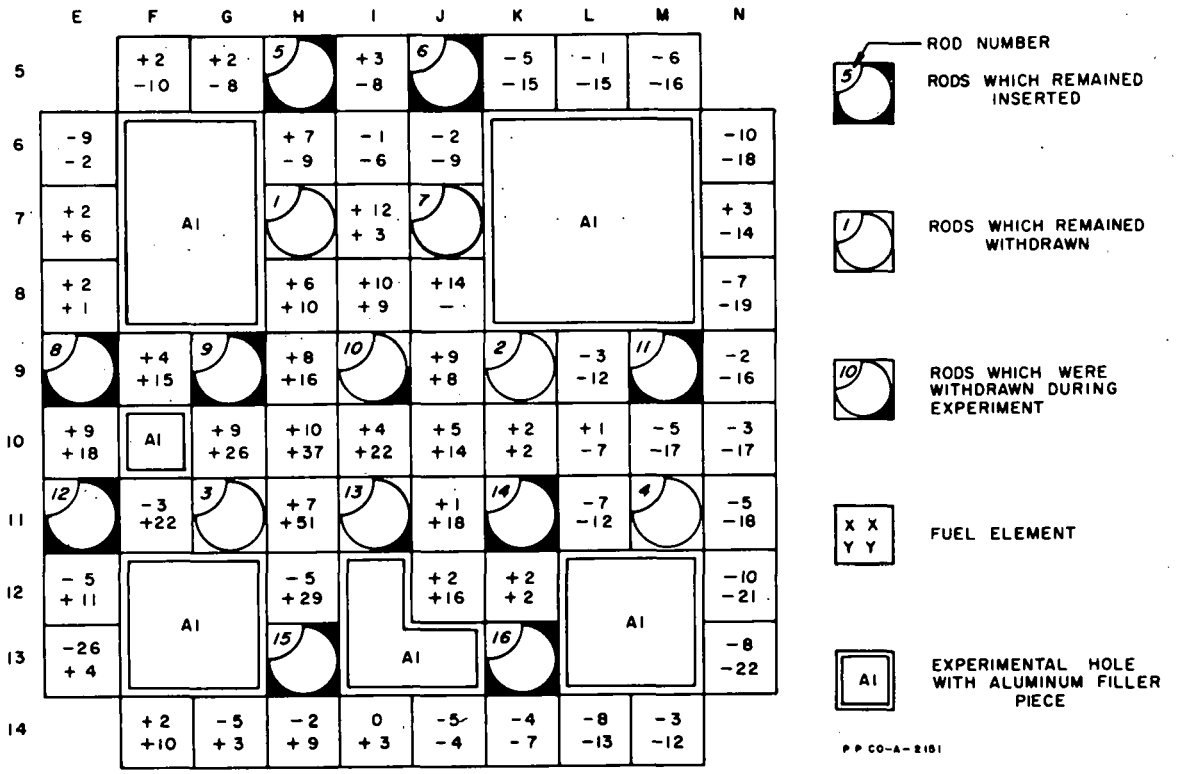

Fig. III-2 Percentage change in thermal neutron flux when Control Rods No. 10 and No. 13 are withdrawn. Top value is change when No. 10 is withdrawn from 18 in. to 36 in. (upper limit). Bottom value is overall change when No. 10 is withdrawn from 18 in. to 36 in. and No. 13 is withdrawn from 0 in. to 36 in.

C. Cycle 13 Loading Mockup (E. E. Burdick, J. W. Henscheid)

Because the ETR core loading for Cycle 13 was quite different from the previous loading and for that matter, from any loading in which a full core flux map had been measured, the loading for Cycle 13 was mocked-up in its entirety in the ETRC. Cycle 6, the first loading in which complete neutron flux distributions had been measured, is very similar to all of the recent loadings; therefore, the differences between that loading and the one for Cycle 13 will be discussed and the neutron flux distributions compared.

The differences between the loadings are as follows:

	Contents of Reactor Position During	
Reactor Position No.	Cycle 6	Cycle 13
C69G7	Al filler and 4 x pieces	GEH-12-1 (without fuel)
C66G13	Al filler and 4 x pieces	GEANP (without fuel)
F10	4 x piece	KAPL
G10	Standard fuel element	ORNL-41
L7 A	Al filler piece	Standard fuel element
M7	Al filler piece	Standard fuel element

In addition, each fuel element in Cycle 13 contained an average of 1.7 gm of natural boron whereas those in Cycle 6 contained 0.75 gm. This caused a large reactivity effect which, when combined with the reactivity effects of the differences just described, changed the initial rod positions considerably. The positions of the rods which were not on the lower limit are as follows:

Cycle 6 - No. 1, 2, 3, 4 at the upper limit (36 in.) and No. 10 at 19 in.

Cycle 13 - No. 1, 2, 3, 4, 10, 13, at the upper limit and No. 6, 8, 11, and 16 at 18 in.

The neutron fluxes for both of these loadings are shown in Fig. III-3. They are compared by showing the percentage difference between the two values in each grid position. It is interesting to note that the flux is much higher on the east side of the core in Cycle 13 than it is in Cycle 6, and that on the west side the opposite is true. Also of interest is that peak flux is lower in Cycle 13 and that it is located in position L10 rather than in J10.

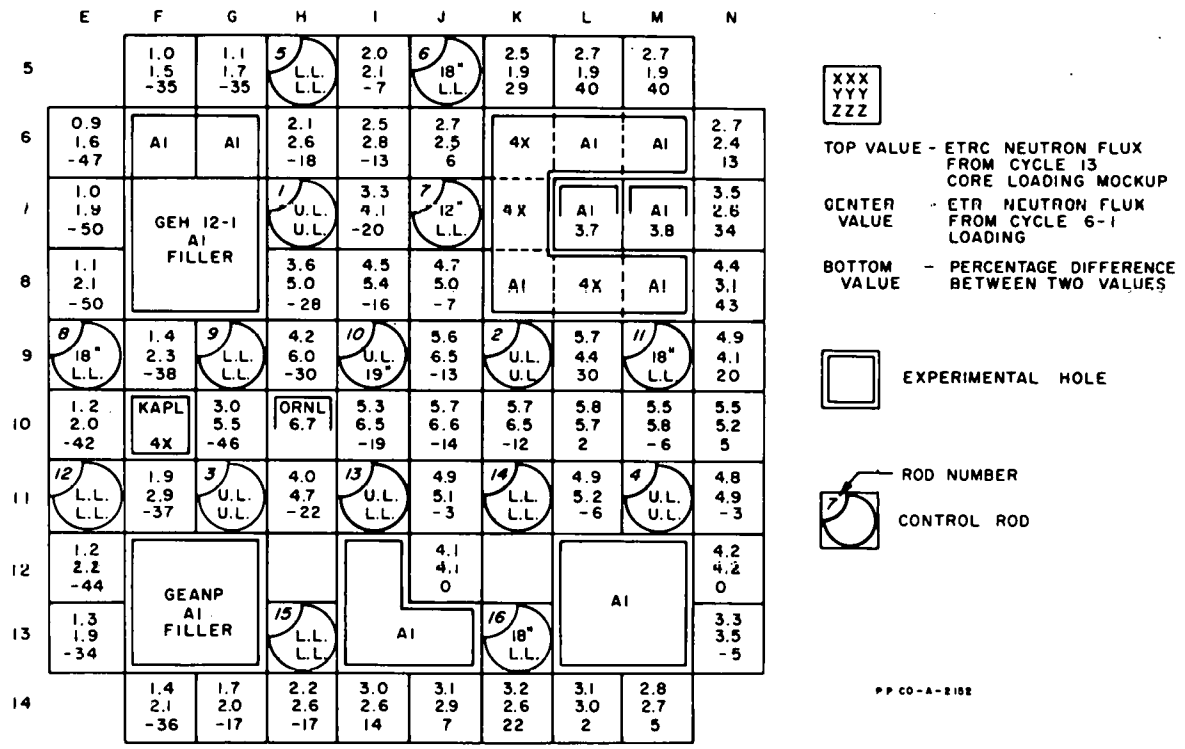

Fig. III-3 Comparisons of ETR Cycle 6 and Cycle 13 horizontal midplane thermal neutron flux distributions. Neutron flux data have been normalized to 175 Mw and are in units of 10^{14} n/cm^2-sec.

IV. REACTOR PHYSICS AND ENGINEERING

A. Radiation Effects on Materials (J. M. Beeston, G. W. Gibson, D. D. Jeffries)

The effect of radiation on materials is being studied by applying testing-type experiments to theoretical relationships with the aim of developing information of both a fundamental and applied nature.

Changes in mechanical strength are presently explained in terms of imperfections--defects, dislocations, etc. The production of defects in metal filaments by irradiation followed by measurement of the change in mechanical strength is one method proposed to extend the fundamental knowledge of radiation effects. Metal filaments (whiskers) are thought to have high strength (close to the theoretical limit) either because of the absence of many imperfections (e.g., only one screw dislocation parallel to the axis of the filament), or because of high strength conditions at the surface (e.g., perfection of the surface, surface films, absorbed impurity atoms, etc.).

The development of techniques to measure the mechanical strength of metal filaments is to the point where it now appears feasible not only to make preliminary selection of a filament by appearance (freedom from bends, kinks, etc.) and by size (less than 10 microns in diameter) but also to make initial bend tests on it so that a lower limit is placed on its strength before irradiation.

The whisker is oriented with a goniometer so that the radius of bend lies in the projection plane of a Model-L Photomicrograph and is then photographed. The diameter of the whisker is measured on a metallograph at 750 X. In Fig. IV-1 an iron whisker whose elastic bending strain proved to be the order of 2% (ratio of whisker radius to bend radius) is shown curved between two holders. This whisker elastically recovered its original shape upon release.

The stability of an intermetallic compound, gadolinium hexaboride, is being studied by pre and post irradiation tests. This material has a special interest as a possible control rod component for high temperature use. Gadolinium hexaboride particles capsulated in an aluminum casting will be irradiated to several levels of integrated neutron flux. The matrix will then be examined metallographically and by x-ray diffraction for particle stability, gas evolution, and bonding effects in relation to the Al capsule.

B. Metal-Water Reactions Program (W. F. Zelezny, D. E. Williams)

Interest in metal-water reactions is stimulated by considerations of reactor safety. In the event of an extreme power excursion or a loss-of-coolant accident in a water-cooled reactor, molten metal could be brought in contact with water or steam with the possibility of an explosive reaction. The purpose of the metal-water reaction study is to determine the conditions under which these reactions are hazardous and to find means of reducing this hazard.

One experimental approach has been to measure the oxidation rates of metals and alloys exposed to water vapor at atmospheric pressure and at temperatures in the neighborhood of 1500 ^{o}F by means of an automatically

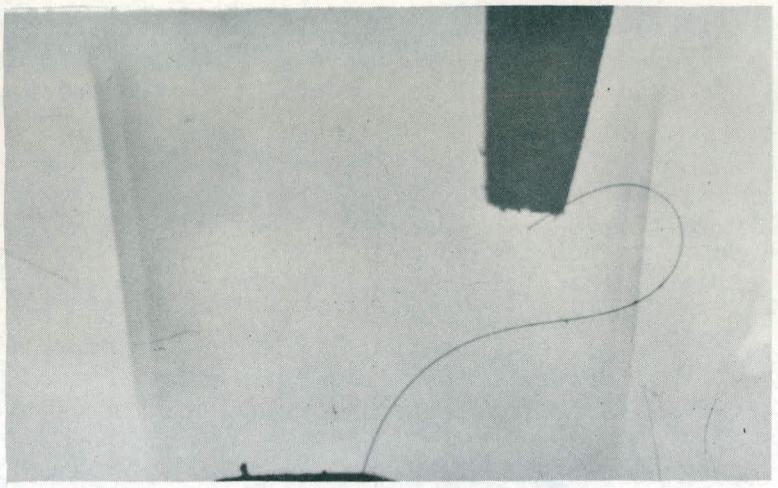

Fig. IV-1 Iron whisker bent to an elastic bending strain of 1.5% (Mag. 23X).

recording thermobalance. Each run was of two hours duration. In every case it appeared that a linear rate law describes the weight gain of the metal with time. The weight gain rates observed to date are listed in Table IV-1.

While low carbon steel is not ordinarily of interest in reactor construction, three runs were made with 1018 steel in order to check the operation of the thermobalance with a material which would show a reasonably high rate of oxidation under these conditions.

For purposes of comparison, two runs were made in which pure Al (99.99%) was exposed to air at one atmosphere and 1507 °F. The reaction rate observed was slightly greater than that with water vapor, which is reasonable to expect. It is interesting to note that the addition of 20 wt-% natural U to the Al approximately doubles the rate of weight gain.

Plans for future work include the obtaining of data at higher temperatures and the calculation of the energies of activation of these metal-water reactions. It is believed that any variable, such as alloy content, which increases the energy of activation of the metal-water reaction will make the reaction more difficult to initiate and thus will act as a safety factor. Equipment combining the induction melting of metals under water and the application of ultrasonic vibration is being set up in an attempt to bring molten metal in contact with liquid water at least momentarily to determine the hazard and violence of the molten metal-liquid water combination.

Table IV-1

RATES OF WEIGHT GAIN FOR SELECTED METALS AND ALLOYS UPON OXIDATION AT ELEVATED TEMPERATURES

Run No.	Metal or Alloy	Oxidizing Atmosphere	Temperature, °F	Weight Gain Rate, $gm/cm^2/min$
3	1100 Al	H_2O Vapor	1470	5.1×10^{-6}
9	99.99% Al		1490	5.3×10^{-6}
11	1018 Steel		1470	6.0×10^{-5}
12	1018 Steel		1470	5.7×10^{-5}
13	1018 Steel		1470	5.6×10^{-5}
16	Al-20 w/o U		1506	12.3×10^{-6}
17	Al-20 w/o U		1500	8.0×10^{-6}
18	Al-20 w/o U		1490	10.6×10^{-6}
21	99.99% Al	Air	1507	10.8×10^{-6}
22	99.99% Al		1504	7.5×10^{-6}

C. Fuel Element Development (W. C. Francis)

In this program, a broad range of fuel materials is under study to further the development of improved fuel assemblies for reactors of the MTR-ETR type. During the quarter, plates containing sample fuel and poison compositions were irradiated to over 60% fuel burnup, and preparations for their post-irradiation metallurgical examination in the MTR hot cell were made. Hydraulic tests were made on a prototype MTR shim rod with removable fuel and poison sections, and on dummy MTR fuel assemblies containing up to 32 fuel plates per assembly. Measurements of the gamma decay dose rate from spent MTR plutonium fuel elements were completed. Transmission measurements were made on the cadmium sections of MTR shim rods to determine the service life of the rods. A vacuum induction furnace, a swaging machine and associated equipment were installed in a sample fabrication laboratory.

1. Sample Fuel Plate Irradiation Program

a. Irradiations (J. M. Waage, O. L. Knighton)

The irradiation tests for phase one of the sample fuel plate program have been completed on 21 compositions having a range of fuel burnup from 10% to 64%. Of this group, 19 plates from ten compositions have been chosen for metallurgical examination in the MTR hot cell. No fission breaks or corrosion into the fuel sections has been observed in the U-alloy or UO_2 compositions, although some surface roughening and corrosion are apparent.

b. Ultrasonic Inspection (J. M. Waage, O. L. Knighton)

Modifications in the ultrasonic equipment are being made to permit its use in the MTR canal for performing non-destructive tests of the fuel plates between reactor cycles to determine bond failure.

c. RMF Measurements (D. A. Millsap, E. Fast)

Measurements on sample fuel plates in the RMF involve (1) pre-irradiation reactivity measurements of all plates; (2) reactivity measurements of selected plates following periods of MTR irradiation; and (3) the evaluation of these measurements. The most nearly identical pair of plates from each composition is selected by means of the pre-irradiation measurements. One plate is retained as an unirradiated standard and the other is subjected to MTR irradiation. The reactivities of the two plates are then compared, following intervals of MTR irradiation. In this manner, the course of the fuel and/or poison burnout with irradiation is followed.

The principal problem in evaluating the reactivity measurements is that of obtaining accurately-known standards for calibration of the statistical weight for fuel and poison at two points in the RMF. The range of fuel and poison content in the sample plates, and the accuracy with which a given plate is known, are not adequate for this purpose. An approximate calibration of the effect of perturbation of the neutron flux has been obtained by using U-235 and boron-impregnated polyethylene tapes next to individual test plates. Some uncertainty is introduced due to the sensitivity of the measurement to the position of the fuel and poison with respect to the plate. The calibration eventually used will be obtained by normalizing these values to analyses for poison and fuel obtained from destructive chemical analysis of selected plates that have been irradiated. In addition, accurately-known standards covering the proper fuel and poison range are being obtained.

Although absolute results on burnout must await accurate statistical weight calibration, values have been calculated comparing the reactivities of the irradiated and unirradiated pairs of plates. Plates containing burnable poison (boron) show an initial increase in reactivity before the fuel burnout becomes the predominant factor, as anticipated.

2. Hydraulic Tests on Experimental MTR Shim Rod (E. H. Porter)

Results of hydraulic tests on an experimental MTR shim rod featuring renewable fuel and poison sections indicate an average coolant velocity of 31.5 ft/sec through the fuel section, with about 65% of the total pressure drop ΔP being measured across the fuel section. The ratio of maximum to average flow velocity is less than 1.1/1.

Since the design requirement for flow velocity is 35 ft/sec through the fuel for adequate heat transfer performance (based upon a proposed 150 gm fuel element), some modifications to the prototype are indicated to reduce the pressure drop at several points along the length of the shim rod. The revised design will require further flow testing and evaluation before in-pile testing is in order.

3. Lifetime Measurements on Cadmium Sections of MTR Shim Rods (G. W. Gibson)

The service life of the cadmium sections of MTR shim rods has been investigated through transmission measurements made on spent shim rods. Sections of Cd taken from fuel-cadmium shim rods (original Cd thickness was 40 mils) that had logged 2545 Mwd of service were still black to a thermal neutron beam, and were not damaged by corrosion. However, the Cd taken from a Be-Cd safety rod (original Cd thickness was 20 mils) with 20,000 Mwd of service was mainly in the form of flakes.

A sample of the flaked Cd was sent to the CPP Analytical Section for analysis by x-ray diffraction. $Cd(OH)_2$ was found to be a major constituent, along with an unidentified crystalline substance. CdO and Cd were found to be minor constituents.

This investigation is to be continued by measuring the transmission of Cd sections of shim and safety rods in service over the range intermediate between the 2000 and 20,000 Mwd values.

4. GCPR Fuel Element Development (W. C. Francis, J. R. McGeachin, E. H. Porter, M. W. Ellingford)

The first of 14 fuel capsules of a statistically-designed irradiation program in support of the Gas Cooled Power Reactor fuel element development program was inserted in an ETR reflector position on February 14, 1959. A detailed description of the program appears in an earlier report.*

Because of the insertion of some large-scale loop experiments in the reactor, the ETR was not brought to full power until March 21, 1959 and then remained at power for only three days before being shut down for further work on experiments. During this brief period of operation, the fuel capsule (MTR-34-2) reached a maximum fuel-can temperature of 1220 °F. By means of flux wires inserted in positions around the fuel capsule for this cycle, the thermal neutron flux was measured for comparison with the heat generation determined by temperature measurements and heat transfer calculations. It is apparent that the design temperature of 1300 °F can be reached only by moving the capsule to a higher flux region.

Except for the thermal barrier system, which was plagued by small gas leaks, the instrumentation and control system performed satisfactorily as designed. Fabrication of additional fuel capsules will be initiated at ORNL as soon as the data from the first capsule has been reduced and evaluated. Increasing the fuel-can temperature to 1600 °F is presently being reviewed. Recent hot channel calculations by Kaiser Engineers--American Car & Foundry indicate that temperatures in the GCPR will probably reach that value.

---

* Francis, McGeachin, Porter, "MTR-ETR Technical Branches Quarterly Report Period Ending September 31, 1958", IDO-16532, 42-43 (1958).

D. Thorium Program (R. G. Nisle)

On four special thorium slugs removed from the MTR July 7, 1958, reactivity measurements have been made in the RMF at intervals over a period of about five months. The analysis of these data is now complete. Because of the lack of appropriate comparison standards, certain assumptions are necessary to make the data amenable to analysis: (1) the decay of Pa-233 to U-233 is essentially complete in five months (approximately 5.5 Pa-233 half-lives); (2) thorium is the only poison present in significant quantities at the end of the five-month decay period; and (3) the loss of Th-232 by conversion to other isotopes during irradiation is negligible.

The results show that the U-233 content can be calculated by either of two methods: (1) by use of reactivity measurements in two positions in the RMF having different relative statistical weighting factors for slow and fast neutrons,* and (2) by use of a previously determined curve** which relates the net reactivity change of the sample in the RMF center position to the total U-233 content. Agreement between the U-233 content determined by these two methods shows that the assumptions (see previous paragraph) are justified.

Table IV-2 presents a summary of RMF measurements and calculations on one of the thorium slugs. The breakdown of the total U-233 content given here is made possible by an analysis of the reactivity transient data.

A least-squares fit of the equation

$$R(t) = (R_\infty - R_o)(1 - e^{-\lambda_{Pa} t}) + R_o \qquad (1)$$

to the reactivity data taken in Positions No. 1 and No. 6 in the RMF was made, where $R(t)$ is the reactivity change resulting from the insertion of the sample into the RMF, R_o is the value of $R(t)$ at $t = 0$, R_∞ is the asymptotic value of $R(t)$ as the time t becomes very large, and λ_{Pa} is calculated on the IBM-650 by an iterated least-squares process. The results are included in Table IV-2.

E. Reactor Physics Constants (R. G. Nisle)

Preliminary measurements of reactivity have been made in the RMF on samples of natural boron, U-233, U-235, thorium, and physicum (a synthetic preparation of stable isotopes that simulates the neutron cross section of fission products). These measurements are being conducted to aid in interpretation of an experiment to determine the effective epi-thermal eta for U-233 relative to that for U-235. The samples were enclosed in cylindrical capsules of stainless steel. Net sample reactivities were measured in two experimental positions with the capsules inside thermal neutron shields.

---

* R. G. Nisle and E. Fast, "Method for Determining the Fission Yield of I-135 with the RMF", IDO-16494 (1954).

** R. G. Nisle and E. Fast, "Progress Report on the Study of Irradiated Thorium", IDO-16402 (1957).

The two cylindrical shields, made of 0.030-in. cadmium and 3/16-in. boron carbide, were designed for 50% transmission of neutrons at 0.50 and 70 ev respectively. Table IV-3 gives a summary of the results compared with reactivities calculated on the basis of a 32-group analysis of the flux in the RMF.* The standard deviation of the measurements based on previous work is estimated to be about 1.0 μk (10^{-6} in δk/k).

Table IV-2

DATA AND RESULTS FOR SPECIAL THORIUM SLUG

U-233 Content of Special Thorium Slug*	Wt. of U-233, gm
From previous irradiation	3.60
Upon removal from MTR	3.75
Produced this irradiation period	0.15
Five months after irradiation	4.08
Summary, Last Three MTR Cycles of Irradiation	
Pa-233 decayed to U-233 (4.08 gm - 3.75 gm)	0.33
U-233 + Pa-233	0.48

Results for Least-Squares Fit of Equation (1)

Quantity Measured	RMF Center Position	RMF Side Position
λ_{Pa}	0.0222 $days^{-1}$	0.0233 $days^{-1}$
λ_{Pa} (literature)	0.0253 $days^{-1}$	0.0253 $days^{-1}$
R_∞	894 μk**	1000 μk
R_o	834 μk	938 μk

* Total weight of slug = 900 gm

** μk = 10^{-6} δk/k

* Theoretical reactivities were taken from calculations made by S. G. Carpenter, Atomics International, reported in a private communication.

Table IV-3

COMPARISON OF CALCULATED AND EXPERIMENTAL REACTIVITIES IN THE RMF

		Reactivity Change, μk*			
		Center Position		Corner Position	
Sample	Wt, gm	Calculated	Experimental	Calculated	Experimental
		Cadmium Shield			
Phys 1	3.679	-2.9	-4.5	-9.2	-12.4
Phys 2	3.768	-3.1	-2.3	-9.9	-7.1
U^{233}	2.841	28.6	22.1	36.4	41.4
U^{235}	3.339	13.1	9.4	15.5	18.0
U^{235}	1.520	6.0	3.5	7.0	8.1
Th^{232}	4.024	-0.23	-2.6	-0.75	-3.6
B-10	1.342	-25.9	-13.8	-80.7	-54.0
B	1.511	-17.0	-7.8	-54.0	-31.6
		Boron Shield			
Phys 1	3.679	-0.86	-0.4	-2.2	+3.3
Phys 2	3.768	-0.88	-1.4	-2.3	+0.4
U^{233}	2.841	4.6	8.1	6.4	54.4
U^{235}	3.339	3.8	6.0	4.8	9.5
U^{235}	1.520	1.7	0.3	2.2	4.4
Th^{232}	4.024	-0.13	0.0	-0.43	0.0
B-10	1.342	-8.3	-4.5	-23.3	
B	1.511	-3.8	-1.4	-11.0	-6.0

* $\mu k = 10^{-6}$ $\delta k/k$.

F. An Automatic Counting System for Gold Foils (R. H. Brown)

An automatic system for counting irradiated gold foils has been built and is now in operation at the MTR counting facility. The system prints on paper tape a measurement of the relative activity of a number of foils, and operates for several hours without attendance.

The equipment makes an automatic decay correction so that the only computation required is multiplication of the raw data output by a constant factor to convert the data into saturated activity. In many cases even this computation is not needed.

The system automatically corrects for decay by setting the length of count for the unknown foil equal to the time required for a standard foil to reach a preset count. The standard foil, irradiated at the same time as the foils to be counted, is placed in a fixed sample holder and counted to a preset count in a separate channel while the foil under study is being counted in the automatic channel. When the count in the standard channel reaches the preset value, the count in both channels is stopped and the accrued count in the automatic channel is printed out. A longer time is required to reach the preset count as the standard foil decays, and this increased counting time compensates for the decay of the foils under study. After printout of the accrued count, both channels reset to zero, the automatic channel changes samples, and the process starts over again.

The major problems encountered during construction of the system involved statistical counting losses and statistical counting errors. The statistical counting losses were due to the arrival of pulses during the dead time of the electronic scalers. Initially the dead time was the order of 10 μsec,* which is equivalent to a counting loss of 1.67% at a counting rate of 10^5 cps. Since an automatic correction for this loss would be difficult to make, ways were sought to reduce it. A modification was designed that brought it down to less than 3 μsec, which is equivalent to a counting loss of only 0.5% at a counting rate of 10^5 cps. These values of dead time were determined by plotting the decay of irradiated indium in the systems' counters. Such a determination of "equivalent" dead time gives a much more realistic dead time than does a determination by the minimum double pulse resolution time technique. Amplifier overload and pulse "pile-up" contributions are not revealed by the latter.

Statistical counting errors arise because of the random nature of nuclear changes. The errors will have a fractional standard deviation of magnitude $\sigma = \frac{a}{N}$ where N equals the total number of counts occuring during any one observation and a is a constant factor depending on the shape of the distribution function. The automatic system makes two such observations for each data point. The computation of the final error is complicated by the fact that it is subject to its own counting error in addition to the counting error introduced by the standard foil. It has been shown that the magnitude of

---

* L. J. Rainwater and C. S. Wu, "Applications of Probability Theory to Nuclear Particle Detection", (Part 2) Nucleonics 2, 42-49 (January 1948).

the final error σ_f is

$$\sigma_f = \sqrt{\left(\frac{a}{N_1}\right)^2 + \left(\frac{a}{N_2}\right)^2} = a\sqrt{\frac{1}{N_1} + \frac{1}{N_2}}$$

where N_1 is the preset number of counts in the standard channel, N_2 is the total count for each foil printed out by the automatic channel, and a is a constant factor from the shape of the distribution function.

G. A Gamma Insensitive Control System for RMF-Type Reactors (S. R. Gossmann)

In reactors operating at "zero power" in the presence of strong gamma fields extraneous to the prompt gamma rays from the fission process, some means of providing a gamma insensitive detector of the neutron flux is desirable. In research reactors such as the RMF where measurements are made by using part of the automatic control system, a gamma insensitive neutron detector is mandatory because so many of the specimens contain highly irradiated fuel. One such detector uses a $AgNO_3$ solution circulated through the reactor, then to an external gamma detector. After measurement, the solution is allowed to decay, then is recirculated in a continuous process.

A simplified version of the proposed gamma-insensitive control system for the RMF has been studied by means of an analog computer. The study was undertaken for two reasons: (1) to determine, in general, the transient response of the controlled reactor and (2) to investigate the variations in reactivity or regulating rod position produced by variations in fluid velocity.

Several simplifying assumptions were made in order that the system could be simulated with the equipment available:

(1) The average instantaneous activation of silver atoms by the neutron flux in the core is the arithmetic mean of the activation at the point where the fluid enters the neutron flux field (inlet) and the point where the fluid leaves the flux field (outlet).

(2) The fluid velocity is composed of two parts--a steady state velocity v_o and a change in velocity with time Δv.

(3) The steady state transit time through the core of each element of fluid is equal to 69.2 sec or two mean lives of the radioactive Ag-110 isotope produced by the neutron flux Φ.

(4) The radioactive decay of the silver atoms is measured at the outlet rather than at some distance from the outlet. (This assumption eliminates a transport lag of the order of 12.5 sec).

(5) The integrating effect of the counter is neglected.

The block diagram of the system simulated on the analog computer is shown in Fig. IV-2. $K_4G_4(s)$ is the simplified transfer function of the gamma-insensitive neutron flux detector relating the change in activation of silver atoms to the change in neutron flux. $K_vG_v(s)$ relates the change in activation of silver atoms to the change in fluid velocity. These transfer functions are defined by:

$$K_4G_4(s) = \frac{N\sigma}{\frac{s}{2\lambda} + 1} = \frac{\Delta q_2(s)}{\Delta\Phi(s)} \quad ,$$

$$K_vG_v(s) = \frac{N\,\Phi_o/2}{\frac{s}{2\lambda} + 1} = \frac{\Delta q_2(s)}{\Delta v(s)/V_o}$$

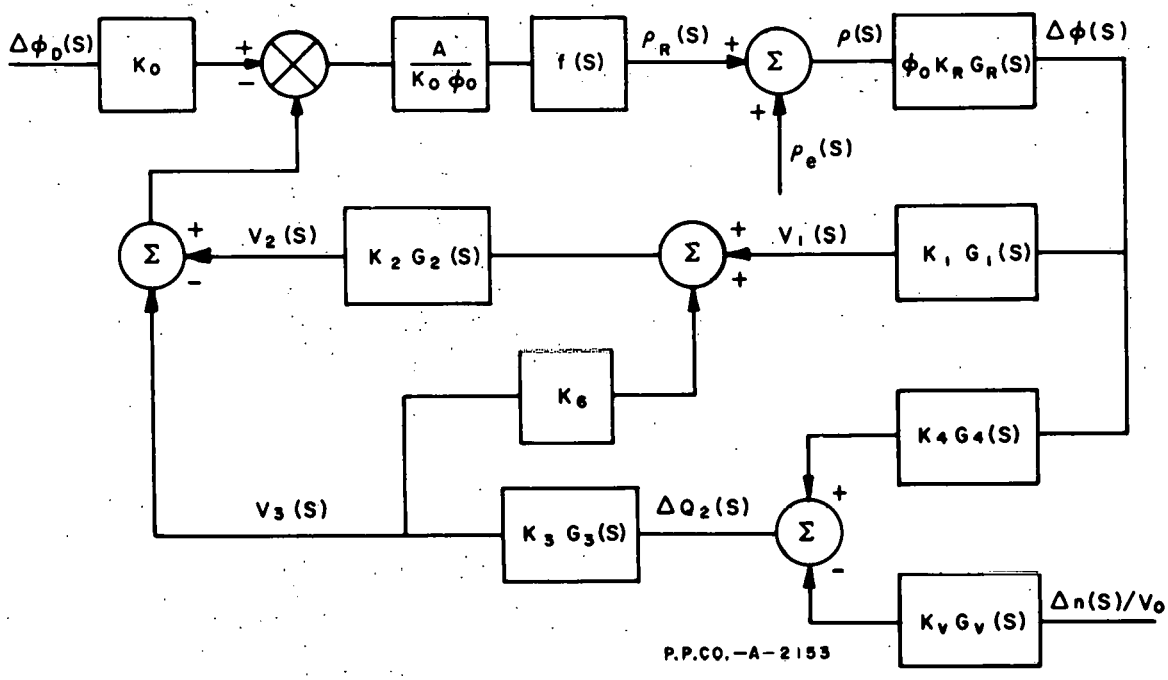

Fig. IV-2 Simplified version of proposed control system for RMF type reactors used in the analog computer study.

The loop containing K_6 has been added to provide damping of a very low frequency oscillation. The other transfer functions in the block diagram were defined in a previous quarterly report.*

To arrive at a desirable transient response, the system was excited by introducing a step in reactivity (ρe). The following values of the control parameters give a stable, well damped response to this type of excitation:

A = 250. volts/volt (amplifier gain)

ξ = 1.2 (damping ratio of servo)

ω_n = 50.0 radians/sec (undamped natural frequency of servo)

$K_1 = 5 \times 10^{-7}$ volts/neutrons/cm^2-sec (ion chamber gain)

K_2 = 5.0 seconds (differentiator gain)

$K_3 = 3 \times 10^{-5}$ volts/pulse/sec (gain of counter)

K_6 = 4.0 volts/volt (amplifier gain)

$\tau_1 = \tau_3$ = 2.0 sec (time constants of ion chamber and counting rate meter respectively)

The variation indicated in reactivity with changes in fluid velocity was found to be of the order of 4.5×10^{-7} $\Delta k/k$ for 1% change in velocity. This figure is, of course, sensitive to the values of the control system parameters. For this reason, a more exact study of the system is proposed. The transport lag and integrating effects neglected in the present study should not be neglected in future studies.

* Gossmann and Moore, "MTR-ETR Technical Branches Quarterly Report, Period Ending September 31, 1958," IDO-16505, 16-17 (1958).

V. NUCLEAR PHYSICS

A. Cross Sections Program (R. G. Fluharty)

1. Thermal Eta Measurement for U-233 (R. G. Fluharty)

Measurements of eta for U-233 with a thermal neutron beam and with monochromatic neutrons in the thermal region, now in the planning stages, will proceed on a high priority basis. A group with appropriate technical specialities has been assembled. The 42-in.-diameter tank is being designed for the $MnSO_4$ bath needed for absolute counting of fission and thermal neutrons.

2. Fast Chopper Total Cross Section Measurements (F. B. Simpson)

a. Thermal Cross Sections (O. D. Simpson, M. S. Moore)

Precise thermal neutron total cross section measurements can now be made with the fast chopper. The procedure developed after extensive studies involves verification by a gold monitor of operating performance at all stages of an experimental run. In effect the chopper is calibrated by measuring the standard sample of gold and comparing results with those obtained under optimum conditions. However, it is not possible to use the gold sample as an absolute standard, since sample thickness is known only to within 1%. A sample with a thickness variation not exceeding 0.5% is being sought.

Neutron cross section measurements in the energy region 0.02-0.08 ev have been taken and are presently being analyzed for the following: Pu-240, U-235, U-233, Au, V, C and B. The 30-mil U-233 sample prepared at Los Alamos has been scanned with the chopper low energy neutron beam and the data are being analyzed to determine the uniformity of the sample.

b. Pa-231 (F. B. Simpson, W. H. Burgus)

Preliminary cross section measurements on Pa-231 have been made covering the energy region from 0.02 to 7 ev. These results show a large double resonance at approximately 0.4 ev with a total of 16 resonances below 7 ev, giving an approximate average spacing between levels of 0.45 ev. The preliminary resonance energies ($\pm$ 1%) are 0.377, 0.492, 0.745, 1.24, 1.97, 2.80, 3.50, 4.13, 4.36, 4.54, 5.06, 5.29, 5.69, 5.88, 6.61 and 6.94 ev.

c. Iridium (M. K. Brice)

Although transmission measurements on the separated isotopes Ir-191 and Ir-193 were not feasible because of the small amounts of sample material, neutron time-of-flight spectra were recorded over the energy range 0.25 to 20 ev. These measurements will facilitate correct isotopic assignment of resonances in this energy region.

In order to calculate cross sections from transmission measurements made with the 45 meter flight path, the observed transmissions must be corrected for the effect of "overlap" neutrons which reach the detectors after a flight time larger than the interval between neutron bursts. The

overlap fraction characteristic of the rotor in use previously* had been measured, but since a different rotor is currently being used, it seemed desirable to carry out a new determination of the overlap fraction and to study its possible dependence on the various types of blanks used to compensate sample holder attenuation of the neutron beam. In theory, the overlap fraction in the open beam could be calculated either from a 16 meter time-of-flight spectrum adjusted to a 45 meter time base, or by comparison of 16 meter and 45 meter spectra. In order to facilitate the extensive numerical calculations involved, and to permit a simple recheck of the overlap fraction under new operating conditions, it is considered advantageous to use automatic data handling methods.

A detailed flow sheet for a program to calculate the overlap fraction by both of the above methods has been prepared and given to the IBM programming staff, by whom the machine program is being written. Results will be reported when the program is operative.

d. Np-237 (J. E. Cline, W. H. Burgus, E. H. Magleby)

Additional transmission measurements as a function of neutron energy for Np-237 have been taken with the MTR fast chopper time-of-flight spectrometer. The samples used in these measurements had thicknesses of 9.45×10^{21} atoms/cm^2, 1.93×10^{21} atoms/cm^2, and 0.898×10^{21} atoms/cm^2. These additional measurements completed the data needed to analyze the resonances and cross section values between 0.01 and 10 ev. Although data have been taken above 10 ev and are currently being analyzed for resonance parameter and cross section values, it is felt that further measurements with the higher resolution rotor are needed to complete the work in the energy region from 10 ev to 1 kev. The Np_3O_8 samples have been analyzed for contaminants, in particular for boron, which may have been introduced during the chemical operations of preparing the sample compound. An upper limit of 0.01% was placed on the amount of B present.

Fourteen resonances were found in Np-237 at energies less than 10 ev. The energies of these resonances are given as 0.489, 1.325, 1.487, 1.975, 3.885, 4.283, 5.891, 6.43, 6.71, 7.53, 8.44, 9.10 and 9.43 ev. The energy values for the low energy resonances now agree with those previously reported from MTR crystal spectrometer data** and ORNL fast chopper data.*** A previous discrepancy in these energies led to the discovery of a systematic error in the chopper time base (see discussion of fast chopper energy scale) which can be important when the rotor is run at low speeds. A level density calculation made with the equations developed by Cameron**** gives a calculated value of 1.55 levels/ev for both spin states, which is to be compared with the observed 1.52 levels/ev.

---

* Fluharty, Simpson, and Simpson, Phys. Rev. 103, 1778 (1956).

** M. S. Smith, et al., Phys. Rev. 107, 525 (1957).

*** G. G. Slaughter, et al., Bull. Am. Phys. Soc. 3, 364 (1958).

**** A. G. W. Cameron, Can. J. Phys. 36, 1040 (1958).

A study of a "shape fitting" technique was undertaken and an analysis scheme evolved that enables analysis of resonances below 10 ev with the IBM-650 digital computer. Approximate resolution functions were calculated as a function of rotor speed and analyzer channel width. These, in turn, were approximated by Gaussian distributions for computational purposes.

3. Fast Chopper Improvements (F. B. Simpson, R. G. Fluharty)

The assembly of the shielded automatic entrance stator sample changer for the fast chopper has been completed. The operating circuitry and mechanical system are being checked out in the laboratory before their installation on the fast chopper.

The BNL shops will begin assembling the new high-resolution four-slit fast chopper rotor on April 6, 1959 and delivery is expected within the month.

4. Cross Section IBM-650 Programs (N. H. Marshall, M. S. Moore)

The Breit-Wigner equation has been programmed for the IBM-650 to facilitate the shape fitting of the cross section data for either a single resonance or a group of 1-10 resonances. A short IBM-650 program was also completed for computing the log of the neutron energy and log of the cross section, and punching out the values in suitable form for plotting on the automatic plotter. A new program for processing the output data from the 1024-channel analyzer has been completed and tested. This program, which utilizes the new features (indexing accumulators and floating decimal arithmetic attachments) of the IBM-650 machine, will cut the processing time required by a factor of three.

5. Fast Chopper Energy Scale (O. D. Simpson, J. E. Cline, and Fast Chopper Group)

The fast chopper energy scale problems now appear to be resolved. In general, they have not been serious for 6,000 rpm operation, and variations which were observed could be attributed to a constant time shift which was due, primarily, to time drift in the delay circuits (saw-tooth time generators or pulsed L. C. oscillator). Present control of this variable is obtained by repeated calibration of the pulsed L. C. oscillator, but a better solution to this problem is anticipated from the development of pulsed crystal oscillators in the Instrument Development Section.

Although the most important factor limiting the use of the chopper as an instrument for absolute energy determination has been instability of the electronic time scale, other contributing factors have become increasingly important at lower rotor speeds, where a constant time shift was found not sufficient to explain discrepancies with other data. Studies extending over some 18 months have led to adoption of the practices and instrument changes enumerated below, which have brought the energy determinations into agreement with crystal spectrometer results:

(1) Careful calibration and monitoring of the delay circuitry in the 1024-channel analyzer, as discussed above.

(2) Determination of the flight path with increased accuracy.

(3) Correction of an inaccuracy in the light triggering system, which gave a variable delay as a function of rotor speed as mentioned in the Np-237 discussion. A method was devised for determining the correction involved, and a new light triggering system is under construction to eliminate this effect.

In general, any time scale uncertainty has been included in the energy errors quoted for the data reported from the fast chopper, since practically all measurements have been made with 6,000 rpm operation and at energies above 10 ev. Whenever a question arose the energy scale was calibrated using known resonances. The only data that have been reported with energies incorrect by an amount slightly greater than the quoted errors, were the low energy U-233 data presented at the 1958 Geneva Conference.* The MTR U-233 data are now in agreement with the total U-233 measurements of V. L. Sailor** at BNL.

6. Monochromating Crystal Studies (R. R. Spencer, J. R. Smith)

A neutron crystal spectrometer produces a monoenergetic beam of neutrons by selecting from the reactor spectrum those neutrons satisfying the Bragg condition for a particular set of planes of the monochromating crystal. At certain orientations there may be other sets of planes in the crystal that also satisfy the Bragg condition for neutrons of the same energy. The resulting competition between planes reduces the intensity of the main Bragg beam of the spectrometer. The observed spectrum shows a series of dips representing orientations where competition exists.

The effects of such competition are being studied with the MTR crystal spectrometer. Curves of counting rate vs. arm angle have been obtained for several planes in Be and NaCl crystals. Many prominent dips appear, particularly in Be, which has a more complicated crystal structure and a higher reflectivity than does NaCl. The planes producing many of these competition dips have been identified by calculations. Be crystals of three thicknesses were used: 0.36, 0.29, and 0.05 inches. The two larger crystals are more nearly perfect and show similar spectra. The thin crystal is smaller in all dimensions, and has a rocking curve showing high multiplicity. Comparison of the spectra produced by the thin crystal with those of the thicker crystals shows a striking phenomenon. While many of the sharp interference dips appear similar in size, shape, and angular position, several others which are prominent in the thick crystal spectra are much smaller and appear to be split in the thin crystal spectrum. It is postulated that the planes responsible for the split competition dips cross twin boundaries in the thin crystal.

---

* Fluharty, Moore, and Evans, "The Total and Fission Cross Sections of U-233 Below 1 Kev," A/CONF.15/P/645, Second International Conference on the Peaceful Uses of Atomic Energy (1958), to be published.

** Private communication.

These studies point out serious difficulties in using crystal spectrometers to measure reactor spectra, and in using smoothed curves for applying order corrections.

B. Nuclear Chemistry (W. H. Burgus)

1. Mass Yields as a Function of Neutron Energy (R. B. Regier, B. H. Sorensen, R. L. Tromp)

The determination of fission yields in Pu-239 and Pu-241 as a function of neutron energy continues. The object of these experiments is to learn whether the ratio of asymmetric to symmetric fission differs between thermal and resonance fission as is the case in U-233[/] and U-235.*,** These ratios are determined by radiochemical measurement of the relative yields of Mo-99, an isotope near the peak of the mass-yield curve, and of Cd-115, Sn-121, and Sn-125, isotopes in or near the valley of the mass-yield distribution. In earlier work with Pu-239 (preliminary results have been presented***) comparisons were made for fission with thermal neutrons and with neutrons filtered through a samarium oxide layer designed to minimize thermal effects and emphasize those of resonance, especially that of the 0.297 ev resonance. Experiments designed to compare the effect of resonance neutrons provided by the MTR crystal spectrometer with that of resonance neutrons provided by in-pile irradiations with Sm coverings remain to be completed. This comparison is necessary to determine the validity of work now in progress on Pu-241 where only the Sm covering technique can be used because of insufficient sample for irradiations with spectrometer neutrons.

Four samples of Pu-239 were irradiated with neutrons of 0.297 ev energy selected by the crystal spectrometer. A determination of the background effects of incoherently scattered neutrons showed that they accounted for only about one fortieth of the fissions observed at 0.297 ev, so they were ignored.

Comparisons of the ratio of asymmetric to symmetric fission may be made in terms of the quantity R defined as

$$R = \frac{A_s'/A_x'}{A_s/A_x}$$

where A is the saturated counting rate for any nuclide, s denotes a standard nuclide (Mo-99 in this case), and x denotes any other nuclide. The A_s/A_x

---

/ Regier, Tromp, and Burgus, "Quarterly Progress Report MTR-ETR Technical Branches", Second Quarter 1958, IDO-16481, 67 (1958).

* LASL Radiochemistry Group, "Resonance Fission of U-235", Phys. Rev. 107, 325 (1957).

** G. A. Cowan and A. Turkevich, "Mode of Neutron-Induced U-235 Fission at Individual Resonances in the Epithermal Region", Bull. Am. Phys. Soc., Series II, 31 (1959).

*** Regier, Tromp, and Burgus, "MTR-ETR Technical Branches Quarterly Report, Period Ending December 31, 1958", IDO-16532, 37 (1959).

term refers to activities associated with thermal neutron fission, and A'_s/A'_x, to activities associated with resonance fission.

The experimentally determined values of R from the MTR crystal spectrometer irradiations of Pu-239 are as follows:

$$R\ (\text{Mo-99: Cd-115}) = \frac{207.0 \pm 17.7\ (4)}{69.0 \pm 2.8\ (12)} = 3.00 \pm 0.28$$

$$R\ (\text{Mo-99: Sn-121}) = \frac{697 \pm 63\ (4)}{212.8 \pm 6.5\ (8)} = 3.28 \pm 0.31$$

$$R\ (\text{Mo-99: Sn-125}) = \frac{219 \pm 4.6\ (4)}{106.6 \pm 3.0\ (8)} = 2.05 \pm 0.07$$

The values in parentheses express the numbers of irradiations and radiochemical analyses on which the adjacent value is based; the uncertainties given are the standard error of the mean. It is interesting to note that the above R values are considerably larger than any previously obtained with U-233 or U-235.

The previously reported experiments with Sm_2O_3 - covered Pu-239 gave erratic results, probably due to leakage of varying amounts of thermal neutrons through thinner portions or "windows" in the powdered samarium-oxide. To provide more uniform Sm covering, the samarium oxide technique has been abandoned, and thin walled Sm metal containers have been fabricated for the irradiations. With these new containers experiments are being carried out to obtain better precision, and to learn whether the integral effect of fission with epi-Sm neutrons is similar to the effect of fission with mono-energetic neutrons at the 0.297 ev resonance.

The effect of neutron energy on the fission mass yields in Pu-241 is also being studied. Pu-241 is similar to Pu-239 in having a strong fission resonance somewhat above thermal energies at 0.27 ev. Because not enough Pu-241 is available to make possible irradiations with the crystal spectrometer, the work is restricted to in-pile irradiations. Approximately 0.5 mg of Pu has been obtained, with the following isotopic composition: Pu-239, 1.10%; Pu-240, 2.18%; Pu-241, 96.60%; and Pu-242, 0.12%. Five thermal neutron irradiations and radiochemical analyses of approximately 22 μgm portions of the Pu-241 have been made, and five irradiations of similar-size aliquots have been completed in the VG-7 facility of the MTR. The thin-walled Sm metal cylinders just described were used to absorb thermal neutrons. Counting of these samples is in progress.

2. Calculation of the Composition of Pile-Irradiated Th-232, U-233, U-235, U-238, and Pu-239 (R. L. Tromp and R. P. Schuman)

Because of the wide interest in the use of U-233 as a reactor fuel and because of growing interest in production of samples of heavy elements for cross section work, a program of calculations was started with the IBM-650 to compute the production of heavy nuclides during the pile irradiation of Th-232, U-233, U-235, U-238, and Pu-239. The calculations are for two typical pile neutron fluxes: the first, typical of the flux seen by MTR fuel, is for

a resonance flux per ln E interval equal to 1/12 thermal flux and with fission flux equal to thermal flux; the other, approximately that seen by the Pu napkin rings whose analyses are available, is for a resonance flux per ln E interval equal to 1/30 thermal flux and fission flux equal to 1/3 thermal flux.

The cross sections used for the calculations are listed in Table V-1.* The cross sections for the Cm, Bk, and Cf isotopes have not been included, since it is planned to fit some of the cross sections to the observed napkin ring yields. The results of the first IBM-650 calculations of the buildup of nuclides in Th-232 (assuming thin sample and resonance flux/thermal flux = 1/12) are given in Table V-2 for a thermal flux of 2×10^{14} n/cm^2 sec. Preliminary hand calculations made for the irradiation of Th-232, U-233, U-235, and U-238 will be used to check the machine calculations.

The hand calculations of the composition of Pu-239 irradiated at 2×10^{14} n/cm^2 sec and reported in the previous quarterly will also be used as a check on the machine calculations.**

3. Studies of Niobium-94 (R. P. Schuman)

Additional studies*** of the decay of 6.6 min Nb-94m and 2.03×10^4 yr Nb-94 have been made. The purpose of this work is to establish the half-life and mode of decay of this nuclide. The 0.50 Mev beta, the 0.703 Mev gamma, and the 0.874 Mev gamma emission rates have been found to be the same, to well within the limit of error of the experiment. This was shown by the use of end-window beta counting using a Cs-137 comparison standard and by absolute gamma scintillation counting. Examination of the gamma spectrum of 6.6 min Nb-94m showed intense Nb K x-rays, a weak 41 kev gamma-ray, and an 874 kev gamma-ray. No 703 kev gamma-ray was seen, but the peak-to-valley ratio of the 874 kev gamma-ray was slightly less than expected, indicating a possible low abundance (< 5%) of the 703 kev gamma-ray. The ratio of K conversion electrons to 41 kev gamma emission is ≈400. If the beta decay of Nb-94m goes to the 1.577 Mev level of Mo-94 in about 2% of the decays, the decay of both isomers is consistent with spin assignments of 0, 2+, and 4+ for the Mo-94 levels, and 6+ and 3- respectively for Nb-94 and Nb-94m.

---

* Cross Section data taken from:
D. J. Hughes and R. B. Schwartz, "Neutron Cross Sections", BNL 325 (1958).
Butler, Lounsbury, and Merritt, CRC-628 (1956).
Bentley, et al., A/Conf. 8/P/809 USA (1955).
T. A. Eastwood, et al., A/Conf. 15/P/203 Canada (1958).
Charpie, et al., "Progress in Nuclear Energy" Series 1, Vol. I, McGraw Hill Book Co., New York (1956).
Hughes, Sanders, and Horowitz, "Progress in Nuclear Energy", Series 1, Vol. II, Pergamon Press, London (1958).
Halperin, Blomeke, and Mrkvicka, Nucl. Sci. Eng. 3, 395 (1958).

** R. P. Schuman, "MTR-ETR Technical Branches Quarterly Report, Period Ending December 31, 1958", IDO-16532, 40 (1959).

*** R. P. Schuman and P. Goris, "MTR-ETR Technical Branches Quarterly Report, Period Ending September 31, 1958", IDO-16505, 69 (1958).

Table V-1

CROSS SECTIONS AND DECAY CONSTANTS USED FOR HEAVY ELEMENT CALCULATIONS

Nuclide	λ, sec^{-1}	Thermal Cross Sections 293 °K Maxwel. Distr. Fission, b	Thermal Cross Sections 293 °K Maxwel. Distr. Capture, b	Resonance Integrals Excl. 1/v Contrib. Fission, b	Resonance Integrals Excl. 1/v Contrib. Capture, b
Th^{232} /	0	0	7.4	0	82
Pa^{231}	0	0	200*	---	---
Pa^{233}	2.93×10^{-7}	0	20 to UX_1 30* to UZ^1	---	470 to UX_1
U^{232}	3.05×10^{-10}	80*	300*	---	---
U^{233}	0	530	61	812	115
U^{234}	0	0	97	0	710
U^{235}	0	576	104	271	50
U^{236}	0	0	6	0	310
U^{237}	1.19×10^{-6}	200**	0	---	---
U^{238} /	0	0	2.71	0	280
Np^{237}	0	0	170	0	600
Np^{238}	3.82×10^{-6}	1600*	0	---	---
Np^{239}	3.43×10^{-6}	0	60*	---	---
Pu^{238}	2.50×10^{-10}	17	454	25	950
Pu^{239}	0	770	338	2000	1600
Pu^{240}	0	0	285	0	8400
Pu^{241}	1.69×10^{-9}	1060	350	(2230)**	(1350)**
Pu^{242}	0	0	23	0	870
Am^{241}	0	2.9	50* to 100 yr 750* to 16 hr	---	---
Am^{242}	2.20×10^{-10}	6400*	1600*	---	---
Am^{243}	0	0	82	0	1580

* Pile cross sections

** Assumed

/ $\sigma_{n,2n}$ = 12.5 mb for Th-232, and 14 mb for U-238.

Table V-2

CALCULATIONS OF THE COMPOSITION OF IRRADIATED Th-232*

Time (days)	Atoms Per 10^6 Initial Th-232 Atoms									
	Th^{232}	Pa^{231}	Pa^{233}	U^{232}	U^{233}	U^{234}	U^{235}	U^{236}	U^{237}	Np^{237}
1.16	999,700	0.25	286	0.0005	4.19	0.26	0.0006	---	---	---
2.32	999,400	0.50	562	0.0020	16.5	1.04	0.0029	---	---	---
4.63	998,800	0.99	1,090	0.0079	64.0	4.12	0.018	---	---	---
8.11	998,000	1.72	1,820	0.024	188	12.5	0.092	---	---	---
11.6	997,100	2.45	2,490	0.048	366	25.2	0.26	0.0020	---	---
23.2	994,200	4.79	4,300	0.185	1,270	96.7	1.96	0.0224	---	---
46.3	988,500	9.19	6,590	0.684	3,840	357	13.7	0.32	0.00089	0.00098
81.1	980,000	15.1	8,160	1.86	7,970	960	60.4	2.58	0.0092	0.0144
116	971,400	20.3	8,720	3.40	11,400	1,718	144	9.16	0.036	0.083
232	943,600	33.3	8,860	9.45	17,000	4,480	611	87.4	0.40	1.89
463	890,400	46.4	8,380	19.5	18,000	8,530	1600	557	2.76	25.7
811	816,100	50.9	7,680	25.6	16,700	10,900	2300	1700	8.68	129
1160	748,100	49.2	7,040	26.1	15,300	11,200	2440	2870	14.8	277

* No self protection assumed. Thermal flux = 2×10^{14} n/cm^2 sec. Resonance flux (per ln E interval) = 1/12 thermal flux. Fast flux (fission spectrum) = 2×10^{14} n/cm^2 sec.

A tentative decay scheme is shown in Fig. V-1. A paper giving the details of the decay scheme work and half-life determination has been submitted for publication.

4. U-235 Alpha Experiment (C. H. Hogg, R. P. Schuman, R. G. Fluharty)

More accurate values of alpha (capture-to-fission ratio) for the reactor fuels are needed for reactor calculations. A determination of the value of alpha for U-235 in a well-thermalized neutron spectrum is being made.* On samples irradiated in the MTR's graphite region, the number of fissions is determined by chemical separation followed by absolute counting of selected fission products. The determination of capture is made by mass analysis.

A second pair of foils irradiated in the graphite region of the MTR now has been dissolved and processed. A third pair of U-235 foils, enclosed in welded copper foil to prevent loss of fission product gas, is currently being irradiated.

For the purpose of calibrating a counter in terms of the number of fissions corresponding to an experimentally measured decay rate of a given fission product (corrected for its decay during and after irradiation), two U samples enclosed in pure Al capsules are now being irradiated in the central portion of the MTR. The number of fissions occuring in these samples will be determined from mass and burnup analyses of the uranium after irradiation. Fission products isolated from these samples then will

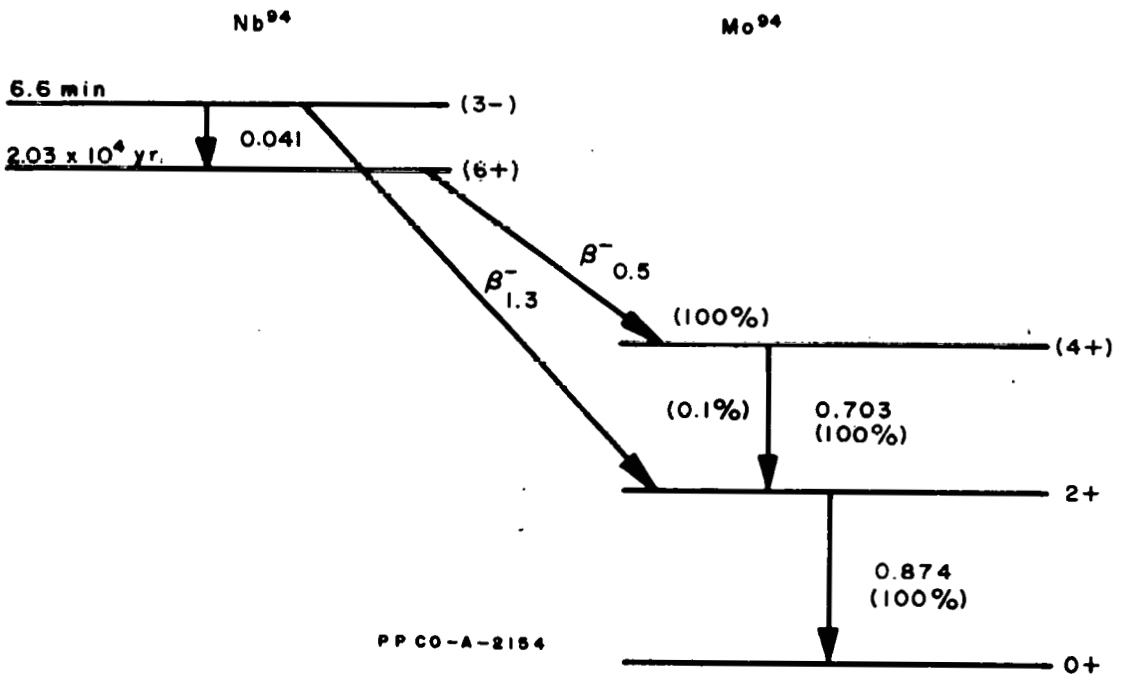

Fig. V-1 Decay Scheme of Niobium-94 (energies in Mev).

* Hogg, Schuman, Fluharty, "MTR-ETR Technical Branches Quarterly Report, Period Ending December 31, 1958", IDO-16532, 38, (1959).

be counted; thus, the counter will be calibrated in terms of the number of fissions which have occurred. With such a calibrated counter, the number of fissions occurring in the samples used for the thermal alpha value determination can be measured through fission product analysis.

5. Pile Neutron Capture Cross Section of Co-60 (E. H. Turk)

The experimental portion of a program begun two years ago to determine a pile capture cross section of Co-60 has been completed. This cross section is of value in determining the optimum irradiation conditions for production of high specific activity Co-60 sources.

Over a period of two years, samples of Co have been irradiated in the MTR L-50 row (where the energy spectrum is approximately the same as that obtaining in MTR production of high specific activity Co-60) for lengths of time varying from 4 to 32 cycles. The Co-60 activities of these samples have been determined and related to the total irradiation received. These data are presented in Table V-3. The total irradiation Φt was obtained from accompanying Co monitors; irradiated for 4 cycles each, removed, and replaced with fresh monitors (this procedure was repeated throughout the 32 cycles). The total irradiation Φt for samples 1 through 8 is thus a summation of the nvt measured by the various individual monitors.

The information presented in Table V-3 has been applied in the following equation in an attempt to obtain a value for the Co-60 capture cross section σ_{60} that gives a best fit to the data:

$$Co^{60} \text{ atoms} = \lambda_{60} N^{o}_{59} \frac{\phi \sigma_{59}}{\phi \sigma_{60} + \lambda_{60} - \phi \sigma_{59}} \left(e^{-\phi \sigma_{59} t} - e^{-(\phi \sigma_{60} + \lambda_{60}) t} \right)$$

where

λ_{60} = decay constant for Co-60

N^{o}_{59} = number of Co-59 atoms present originally

ϕ = neutron flux (n/cm^2 sec)

σ_{59} = thermal capture cross section of Co-59

σ_{60} = effective pile neutron capture cross section Co-60

t = irradiation time

As a first approximation in determining σ_{60}, the average flux for the whole irradiation program was used in the above equation. This treatment gave a value of 34 barns for σ_{60}. A more refined calculation, in which corrections for reactor shutdowns and flux variations are being applied, is underway. An IBM-650 program is being written.

Table V-3

Co-60 PRODUCTION AS A FUNCTION OF Φt

Sample Number	Integrated flux $\Phi t(n/cm^2 \text{ sec} \times 10^{21})$*	Irradiation time $t(\text{sec} \times 10^{-7})$	Co-60 Activity $(d/\text{sec/mg} \times 10^{-9})$
1	1.99	0.47	2.47
2	4.66	1.25	5.77
3	6.34	1.81	7.56
4	7.49	2.21	8.68
5	9.65	2.59	10.7
6	11.14	3.12	11.6
7	12.37	3.62	11.5
8	13.81	4.13	11.9

* From summation of cobalt monitors

C. Inelastic Scattering of Slow Neutrons Program (R. M. Brugger)

This program is being set up to measure the energy and angular distributions of neutrons scattered from reactor moderator and reflector materials as functions of incident neutron energies (below 1 ev) and material temperature. Preliminary results of scattering at 90° from steam, methane, vanadium, nickel, beryllium, water, and heated samples of graphite have been obtained (Fig. V-2 is a pictorial drawing of the velocity selector used for these measurements). Multiple angle detectors and the 1024-channel time analyzer were installed and background studies were begun.

1. Inelastic Scattering Data for Steam, Methane and Vanadium (R. E. Schmunk)

The MTR velocity selector and a 100-channel time analyzer were used to measure the energy of neutrons scattered at 90° from samples of methane, steam, and vanadium. By proper choice of the operating parameters of the velocity selector, bursts of monoenergetic neutrons at several energies were obtained. When these neutrons hit the sample some were scattered to the detectors. The times for the neutrons to travel from the sample to the detectors were measured to determine whether or not the neutrons had gained or lost energy during the scattering process.

The CH_4 and steam were contained in 1/16-in. wall Al cans 3 in. in diameter by 6 in. high, evacuated before introduction of the samples. The CH_4 pressure was 102 psig in one test, 62 psig in another. The steam pressure resulted from about 2 gm of water heated to 175 °C.

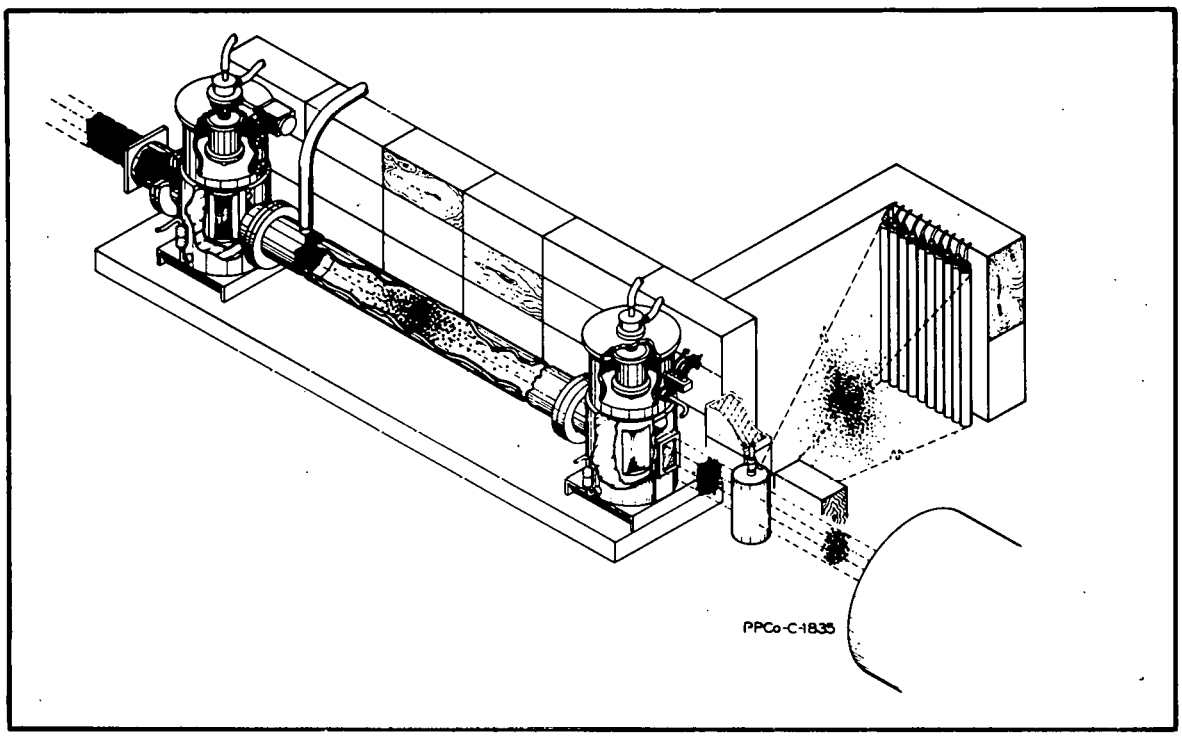

Fig. V-2. MTR Neutron Velocity Selector. The neutron beam from the reactor proceeds from the left to the first rotor. The neutron burst from the first rotor spreads out as it travels to the second rotor which transmits a monoenergetic burst of neutrons. Some of these neutrons (< 15%) are scattered in all directions by the sample. The energies of those going to the BF_3 detectors are measured by time-of-flight electronics.

The data obtained were in the form of a counting rate per time channel. After corrections for background, counting loss, and counter efficiency were made, a differential scattering cross section was calculated. Figs. V-3 to V-8 show data for methane for seven values of the incident neutron energy and Figs. V-9 to V-14 apply similarly to steam. The differential cross section per angle and per energy interval of the neutrons for scattering is plotted against the neutron wavelength. Since vandium has been shown to have very little inelastic scattering, scattering from a 0.188-in-thick vanadium metal sample was used to determine the energy resolution of the incident neutrons. The solid curves show these data. The sharp peaks show the resolution of the velocity selector. The broad tails on each side of the main peak are due to neutrons inelastically scattered from vanadium.

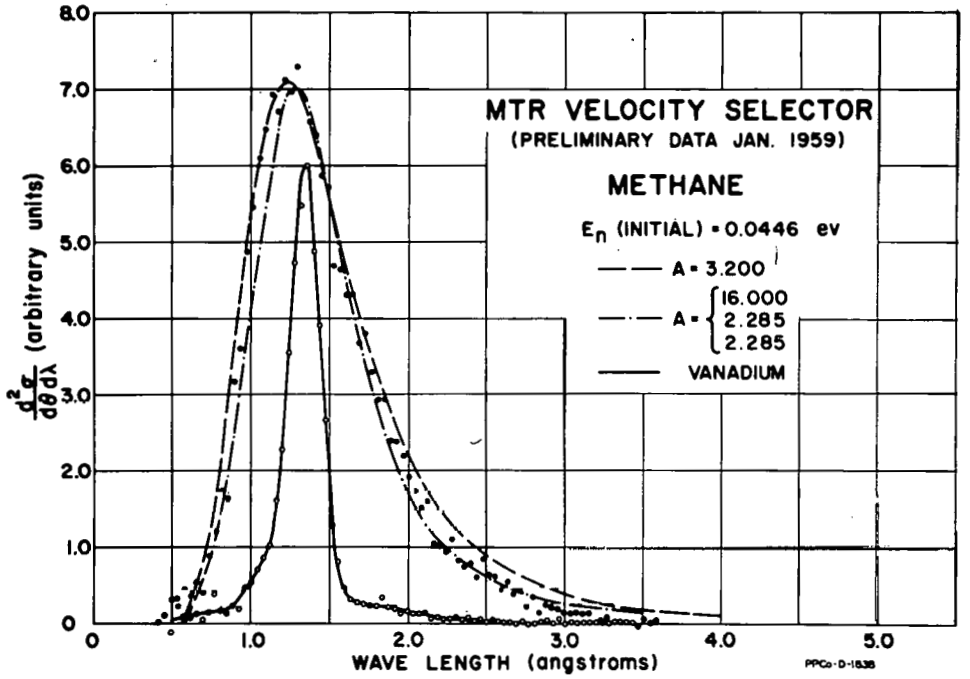

Fig. V-3 The scattering of 0.0446 ev neutrons from methane.

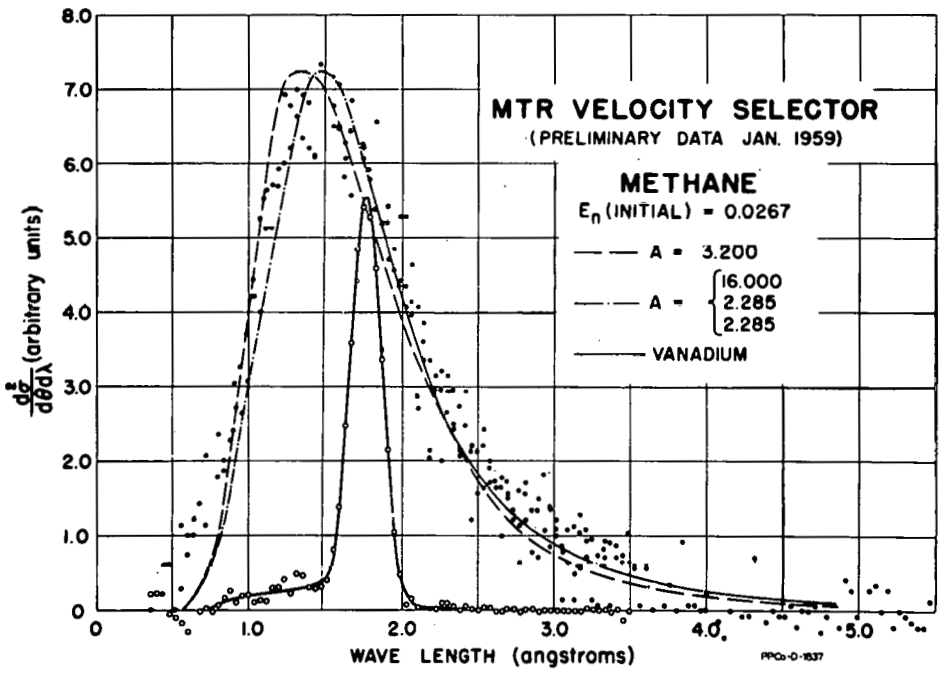

Fig. V-4 The scattering of 0.0267 ev neutrons from methane.

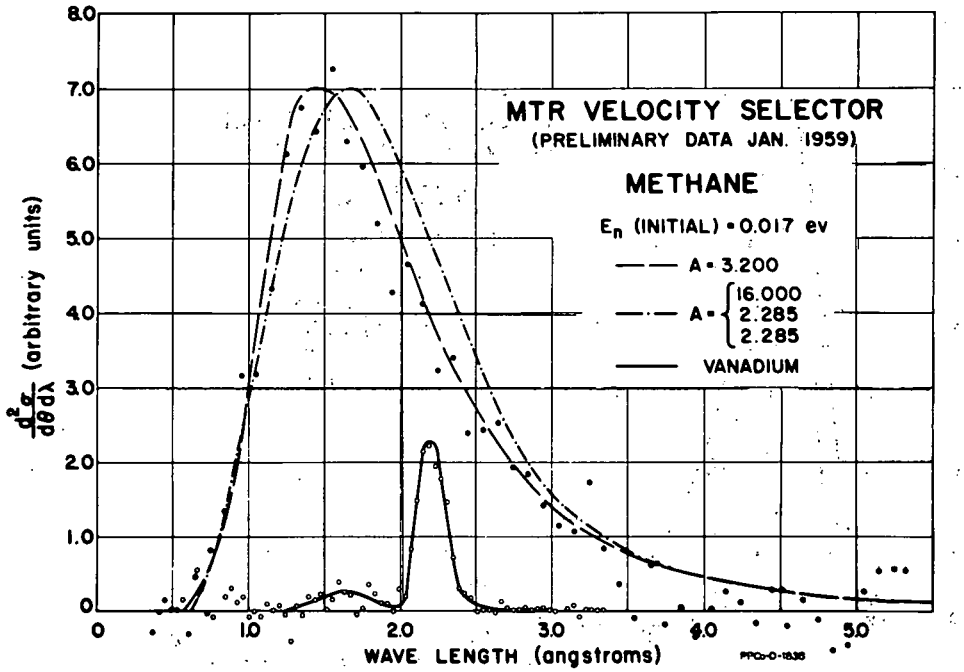

Fig. V-5 The scattering of 0.017 ev neutrons from methane.

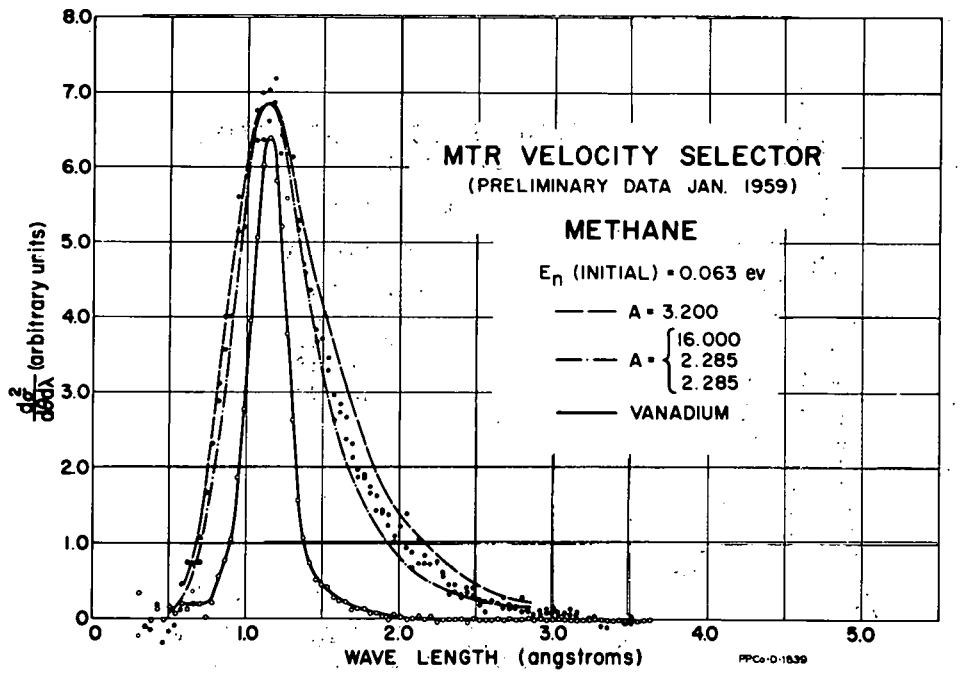

Fig. V-6 The scattering of 0.063 ev neutrons from methane.

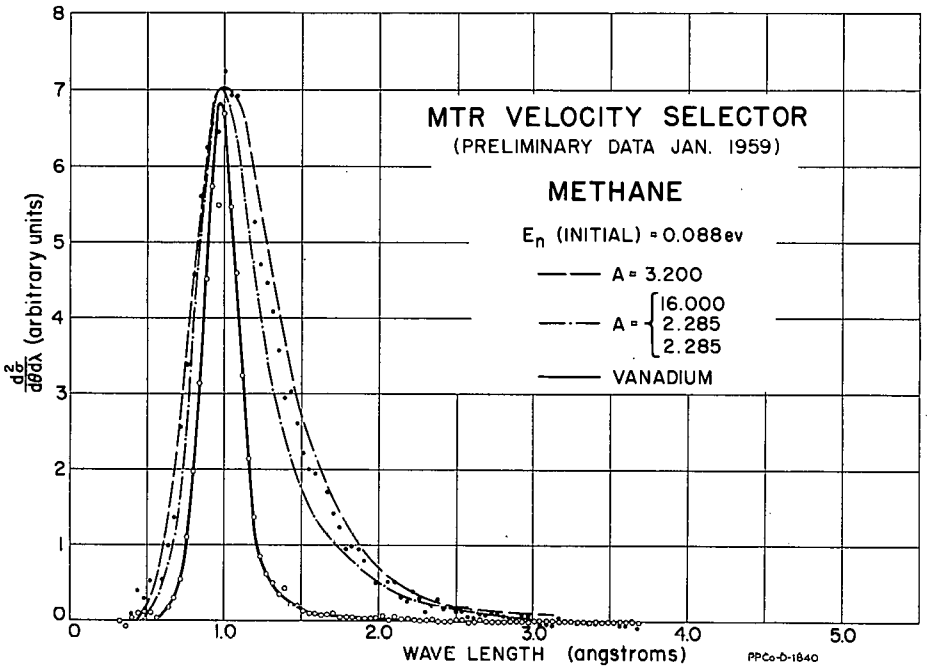

Fig. V-7 The scattering of 0.088 ev neutrons from methane.

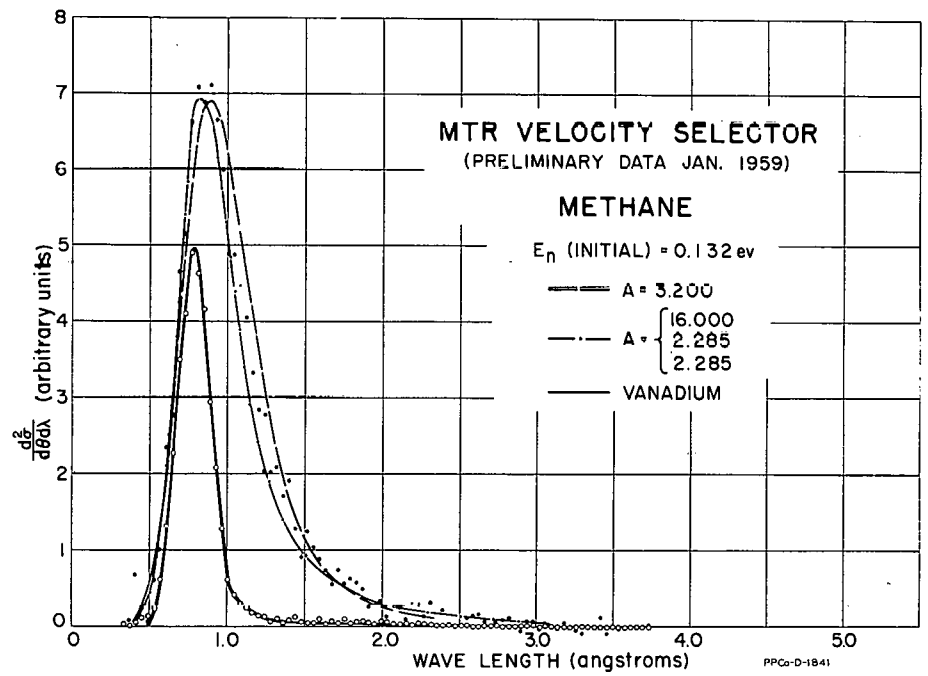

Fig. V-8 The scattering of 0.132 ev neutrons from methane.

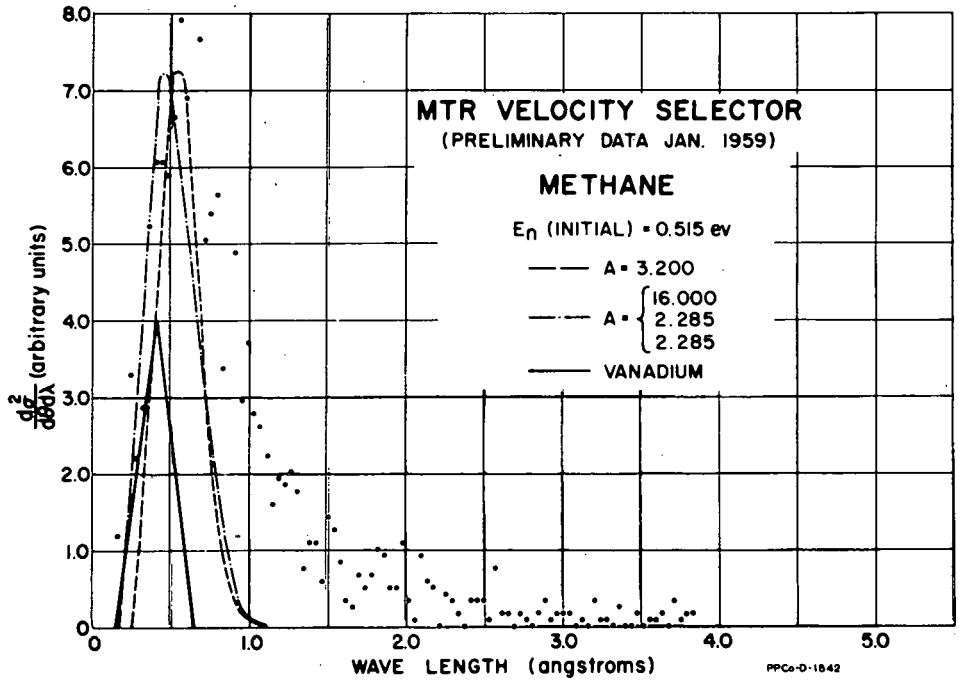

Fig. V-9 The scattering of 0.515 ev neutrons from methane.

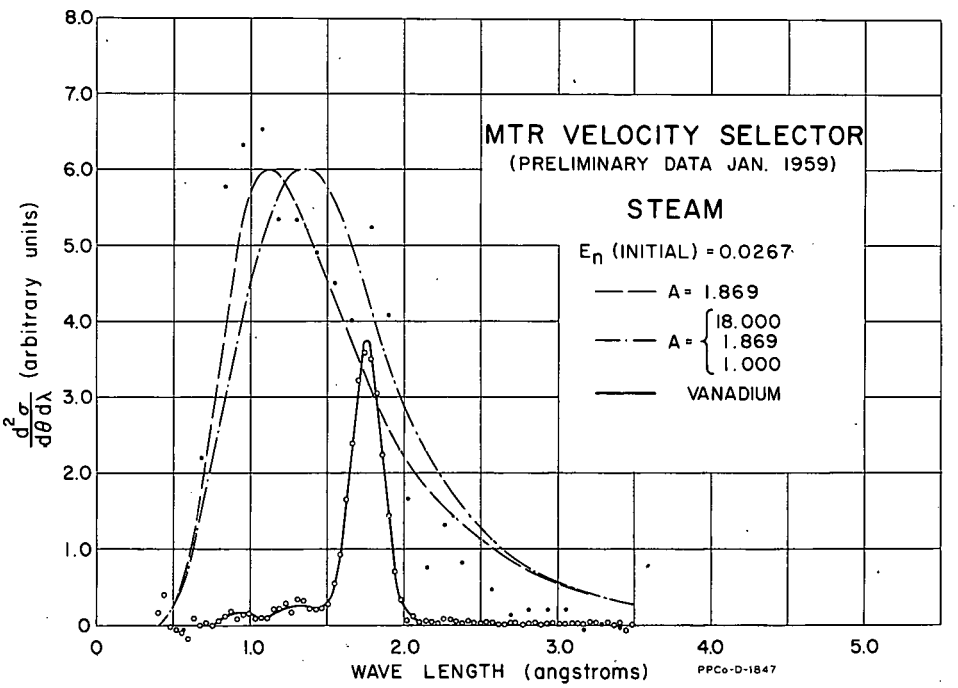

Fig. V-10 The scattering of 0.0267 ev neutrons from steam.

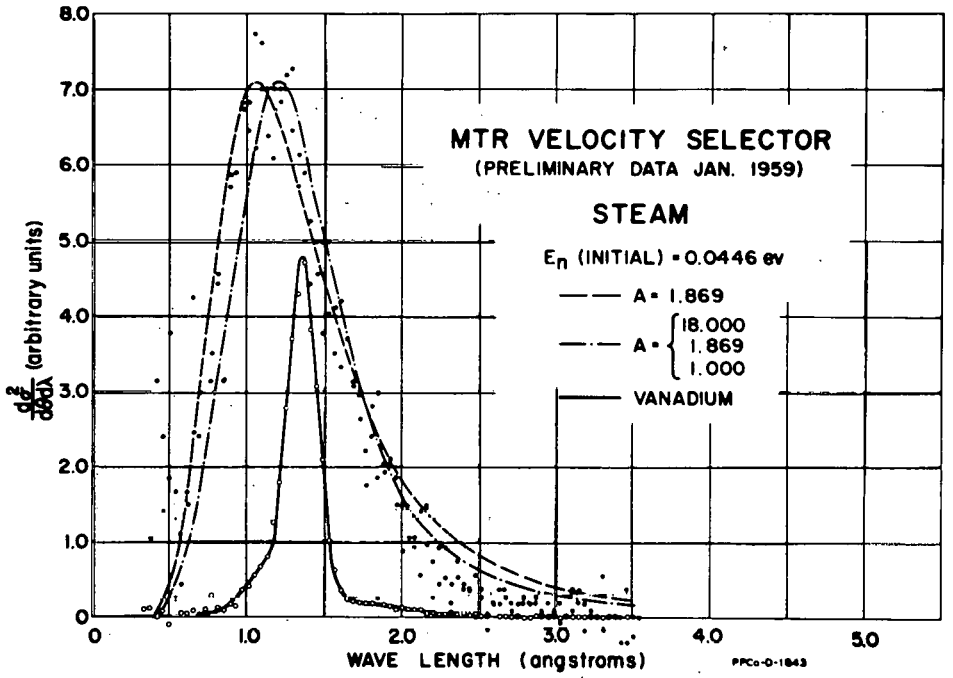

Fig. V-11 The scattering of 0.0446 ev neutrons from steam.

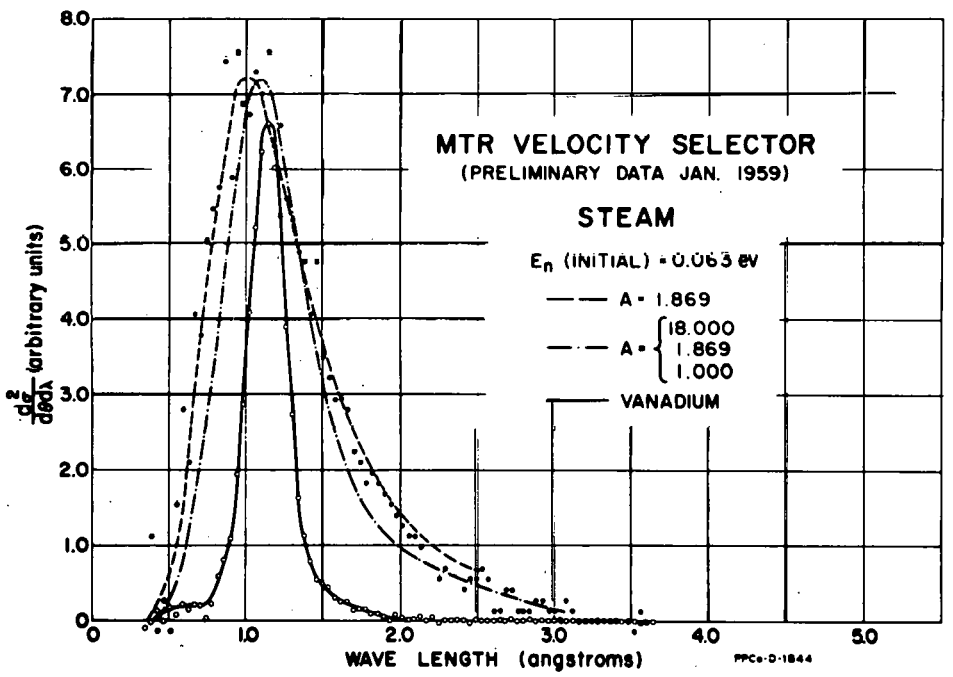

Fig. V-12 The scattering of 0.063 ev neutrons from steam.

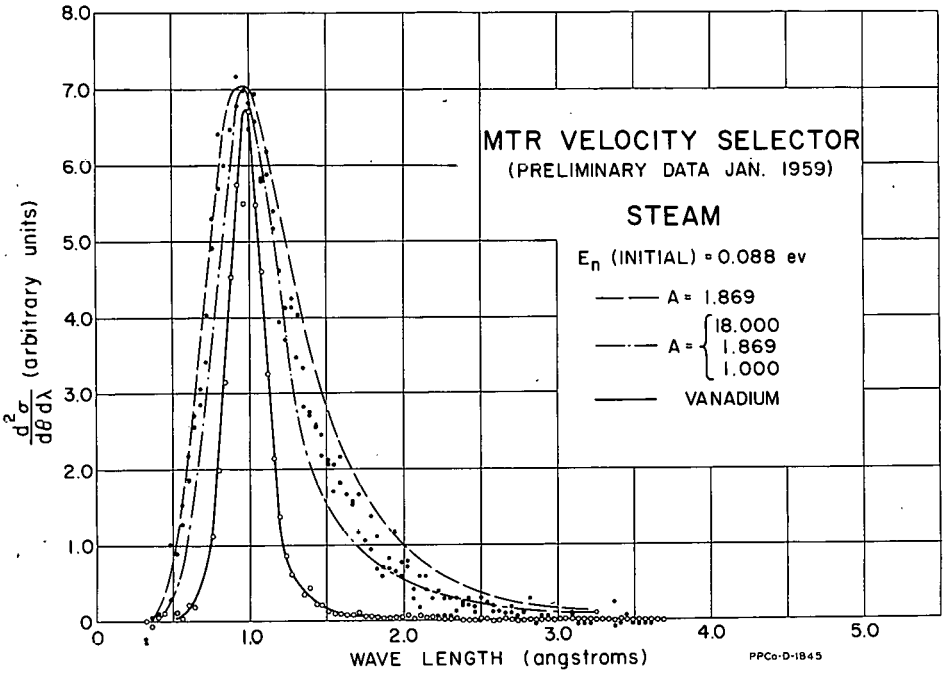

Fig. V-13 The scattering of 0.088 ev neutrons from steam.

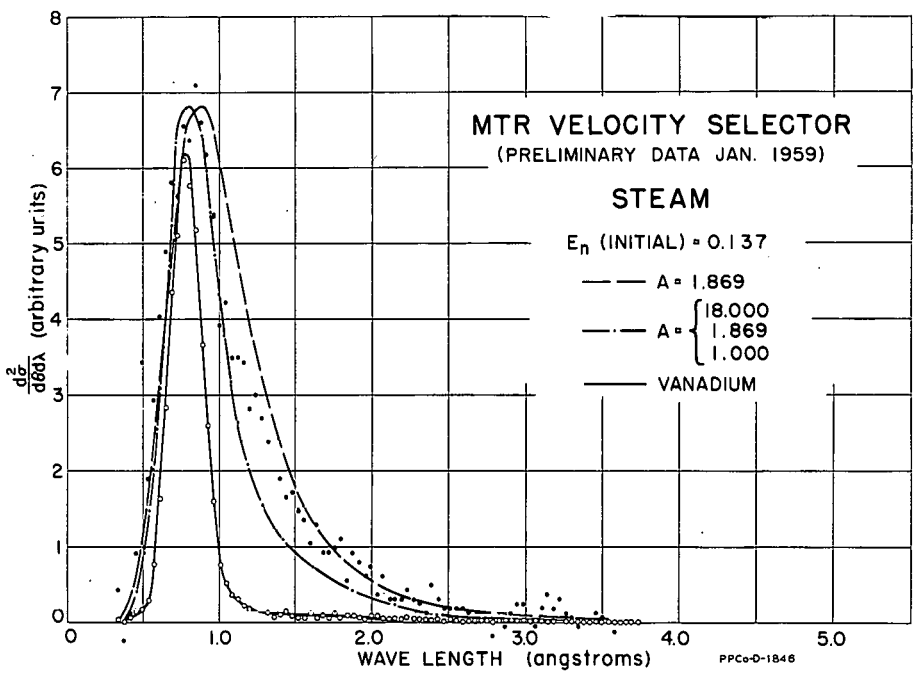

Fig. V-14 The scattering of 0.137 ev neutrons from steam.

Sachs and Teller* have suggested that the scattering of neutrons by molecular gases can be approximated by scattering from mass points, provided the mass points have the appropriate mass tensor components. Spiers** has derived an equation yielding the differential scattering cross section per angle and per energy interval for neutrons scattered from mass points having a Maxwellian distribution of velocities. An attempt has been made to fit the data through a combination of these results. Two of the more satisfactory approaches are: (1) a gas composed of three equal parts by number, each part having gas atoms with masses equal to the reciprocal of one of the mass tensor components, and (2) a gas composed of atoms with one mass, the mass being the reciprocal of the average of the mass tensor components.

In each of the figures, the theoretical fits to the experimental data are given by the broken (dashed and dashed-dot) curves. The dashed curve is the shape fit for the average mass tensor gas; the dash-dot curve is the fit for the mixture of three gases. In each legend, the values in the bracket are the reciprocal mass tensor components. (Because of the symmetry of the CH_4 molecule, two of its mass tensor components are the same).

The fits for most incident energies follow the same pattern. The average mass tensor curves (dashed lines) give better fits on the high energy side, and the curves based on the mixture of the three gases (dash-dot lines) give better fits on the low energy side. However, the data are not accurate enough to accept or preclude either fit.

Magnitudes for the cross sections were computed from data obtained with a crude flux monitor. These cross sections fell 20 to 40% below the values predicted by the theories, but they agreed within the experimental error. A comparison of the fits and magnitudes of the cross sections, both for steam and methane, indicate a slight preference for the average mass tensor approach.

2. Preliminary Measurements on Graphite, Water, Nickel, and Beryllium (R. E. Schmunk)

Preliminary data for neutrons scattered at 90° from graphite samples were taken with sample temperatures of 27, 300, 450, and 600 °C. The graphite samples burned at the higher temperatures, so an evacuated sample container will be needed to extend the data to higher sample temperatures. Survey measurements have been taken on Ni and Be. Following the installation of multiple angle detectors and the 1024-channel analyzer, measurements were started on scattering from a 0.010-in.-thick water sample over a temperature range from 40 to 100 °C.

3. Mechanical Modifications of Velocity Selector (P. D. Randolph)

Velocity selector resolution has been greatly improved by the set of curved slits installed in the two rotors. Neutron tests have shown that

---

* R. G. Sachs and E. Teller, Phys. Rev. 60, 18 (1941).

** J. A. Spiers, National Research Council (Canada) Report CRT-417, NRC No. 1940, (April, 1949) unpublished.

expected transmission characteristics and counting rates have been achieved. Bursts of shorter duration can now be obtained at the lower energies without the intensity loss that accompanies this mode of operation with straight slits. Curvature of the slits (radius of curvature is 84 in.) is such that intensity is maximized at the peak of the Maxwellian when the rotors are spinning at 6000 rpm.

Equipment for experiments on multiple-angle scattering is being installed and tested. Multiple counter banks subtending a total angle of 80° from the central target position have been placed within a circular shielding room. There are 8 such banks, located 10° apart on a 2 meter radius. Each bank is a row of ten BF_3 proportional counters (active length 20 in., diameter 1 in., gas pressure 120 cm).

Walls of the shielding room are made up of steel tanks filled with borated paraffin. The tanks, 6-1/2 ft. high, 4 ft. wide, and 1 ft. thick individually, have shiplap edges so that they line up to form a continuous wall having a radius of 81 in. Roof shielding consists of boxes filled with borated paraffin to form a 6-in. thickness. The inside surface of roof and walls is lined with 0.020-in.-thick cadmium.

Upon completion of the room, background measurements were made. Neutron tests showed that backgrounds produced by fast neutrons which passed through the first rotor and scattered from the second were appreciable. A factor-of-five reduction was achieved by installing Cd-lined, 12-in.-thick borated paraffin walls along the two edges of the 80° sector, but further reduction is desirable. Improved shielding, filters, and collimation are being sought.

4. Electronic Modifications of Velocity Selector (L. W. McClellan, R. B. Kennedy)

Operation of the single phase 1800 rpm hysteresis motors as two-phase variable speed motors from 1000 rpm to 6000 rpm is allowed by a newly developed circuit which employs control transformers instead of capacitors to set the 90° phase shift. The three-phase output from the variable frequency oscillator is applied to the transformer circuit and two phases with a 90° shift between them are taken out of the circuit and amplified by 200 w McIntosh power amplifiers. The voltages of the two phases are then balanced and applied to the two hysteresis motors driven simultaneously by this system. The instantaneous phase relationship of one motor with regard to the other holds better than 3' of arc at most speeds.

A major shifting of electronic control and detector equipment coincided with the installation of the 1024-channel analyzer, to make room for detectors and shielding. A total power magnetic circuit breaker was installed, and the rewiring of all the circuits was completed and checked out.

D. Decay Schemes Studies

1. The Decay of 23 min Sm-155 (R. L. Heath, D. G. Proctor, C. W. Reich, E. C. Yates)

a. Introduction

The only detailed investigation of the radiation associated with the decay of the 23 min samarium activity is that reported by Ruthledge, Cork, and Burson*. This work included investigations of beta-ray and conversion electron spectra, and coincidence studies. From the results of their measurements a level scheme for Eu-155, consistent with the observed data, was constructed. The proposed scheme included levels at 0.105 and 0.351 Mev. Two gamma-rays, emitted with equal intensity, were observed at 0.105 and 0.246 Mev. A single beta-ray of 1.8 Mev was reported leading to the 0.351 Mev level.

Observations of the radiations from the 23 min Sm-155 activity, made here during preparation of a source of 15 day Eu-156 by neutron irradiation of magnetically separated Sm-154, indicated that the previously reported information on the decay of this nuclide was in large part incorrect. The Eu-156 nucleus, with 88 neutrons and 63 protons, lies in a region of highly deformed nuclei. In this region the collective model** has been very successful in predicting the energies and spins of the low-lying levels. Upon application of the collective model to this nucleus, the predicted levels did not agree with the previously reported data. To remove this discrepancy, a more detailed study of this nuclide was undertaken. Preliminary results are presented in Fig. V-15.

b. Source Preparation

Sources of the 23 min Sm-155 activity were prepared by irradiation of magnetically separated Sm-154 in a high flux facility of the MTR. The purity of the source material was assured by following with scintillation spectrometers the decay of both gamma and beta radiation. The only contamination indicated was from 47 hr Sm-153 produced by neutron activation of Sm-152 present in the mass-separated material. Upon removal from the reactor this activity was less than 5% of the total source strength. Point sources (0.1 cm in diameter) were prepared on thin films (10 mg/cm^2) for photon counting.

c. Gamma-Ray Measurements

The gamma radiation emitted in the decay of Sm-155 was observed with 3 in. diam. by 3 in. cylindrical NaI(Tℓ) detectors. Sources were measured in point geometry, at 10 cm on the vertical axis of the detector, to

* Ruthledge, Cork, and Burson, Phys. Rev. 86, 775 (1952).

** A. Bohr, and B. R. Mottleson, "Kgl. Danske Videnskab," Selakab, Mot. fys. Medd. 27, No. 16 (1953).

reduce "coincidence summing" in the detectors. Polystyrene absorbers (1.3 gm/cm^2) were interposed between source and detector to remove the beta radiation. All measurements were made in a large detector shield with inside dimensions of 32 in. by 32 in. by 32 in. to insure that scattered radiation would not cause any complications. The scintillation spectrometers were energy-calibrated by the usual method of "internal comparison" to reduce the effect of rate-dependent gain fluctuations in the photomultipliers and pulse amplifiers. Sources of Bi-207 (Pb x-rays) and Ce-141 (0.142 Mev) were used for this purpose.

A typical pulse-height spectrum obtained from Eu-155 is shown in Fig. V-15. Gamma-rays were observed at 0.105 ± 0.005, 0.142 ± 0.005, and 0.245 ± 0.005 Mev, together with Eu K x-rays associated with internal conversion of the gamma-rays. The decay of the sources was followed for a period of four half-lives. All gamma-rays exhibited a decay period of 23 ± 2 minutes.

Relative intensities of the gamma-rays were obtained by successive subtraction of pulse-height distributions representing the response of the detector to monoergic radiation, as described in IDO-16408.* The results of these analyses are given in Table V-4.

d. Coincidence Measurements

The energies and relative intensities obtained from the gamma-ray analyses suggested levels at 0.106 and 0.245 Mev, with the 0.245 Mev gamma-ray crossing over the 0.142 and 0.106. In addition, the principal beta-ray branch is to the 0.106 Mev level, with only minor branching to the second excited state.

To verify this level scheme, gamma-gamma coincidence measurements were made using a pair of 3-in. by 3-in. NaI (Tℓ) detectors. The detectors were mounted with their axes in a horizontal line with a spacing of 6 cm. "Graded" backscatter shields were used to reduce false coincidence effects due to scattering of gamma-rays between the detectors. The coincidence circuitry was of the "fast-slow" type with a fast resolution of 6 x 10^{-7} sec. The coincidence spectrometer consisted of an automatic sliding-window, single-channel analyzer operated in coincidence with a fast 100-channel discriminator-type analyzer.

Coincidence spectra were obtained with the single-channel analyzer adjusted to accept only pulses from the "photo-peaks" of the 0.106, 0.142 Mev, and 0.245 Mev gamma-rays.

The results of these measurements are shown in Fig. V-16 and V-17. From these data it is apparent that the 0.106 and 0.142 Mev gamma-rays are in cascade with the 0.245 Mev gamma-ray crossing over to the ground state. These coincidence data, together with gamma-ray energies and relative intensities, are considered to be reasonable confirmation for the two low-lying levels in Eu-155.

---

* R. L. Heath, "Scintillation Spectrometry Gamma-Ray Spectrum Catalogue", IDO-16408 (1957).

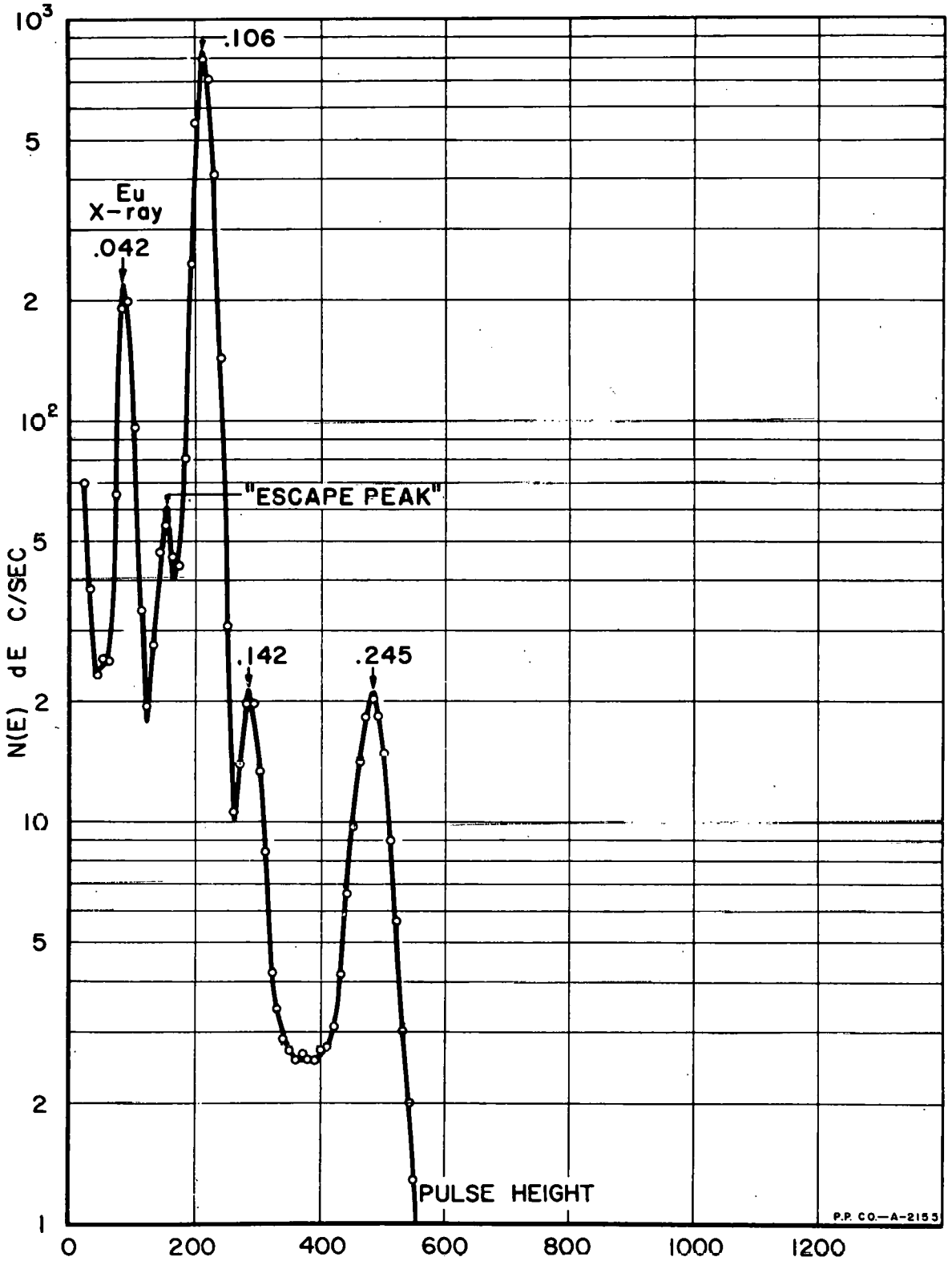

Fig. V-15 25 min Sm-155. 3 in. x 3 in. - 2 NaI. Absorber - 950 mg/cm^2. Source distance - 10 cm(c). Energy scale ≈ 0.5 Kev/PHU.

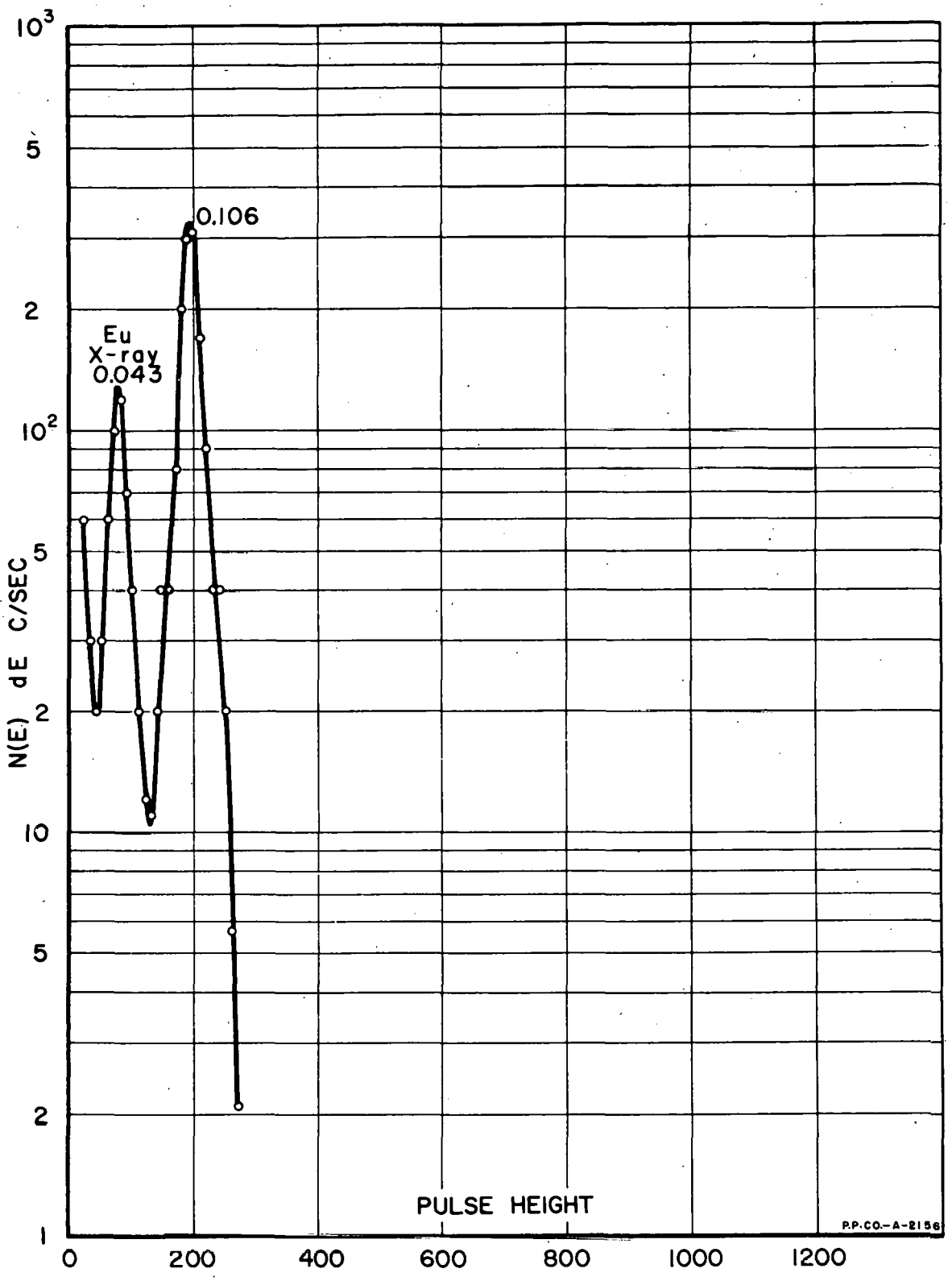

Fig. V-16 Coincidence gamma-ray spectrum showing radiation in coincidence with 0.142 Mev gamma-ray.

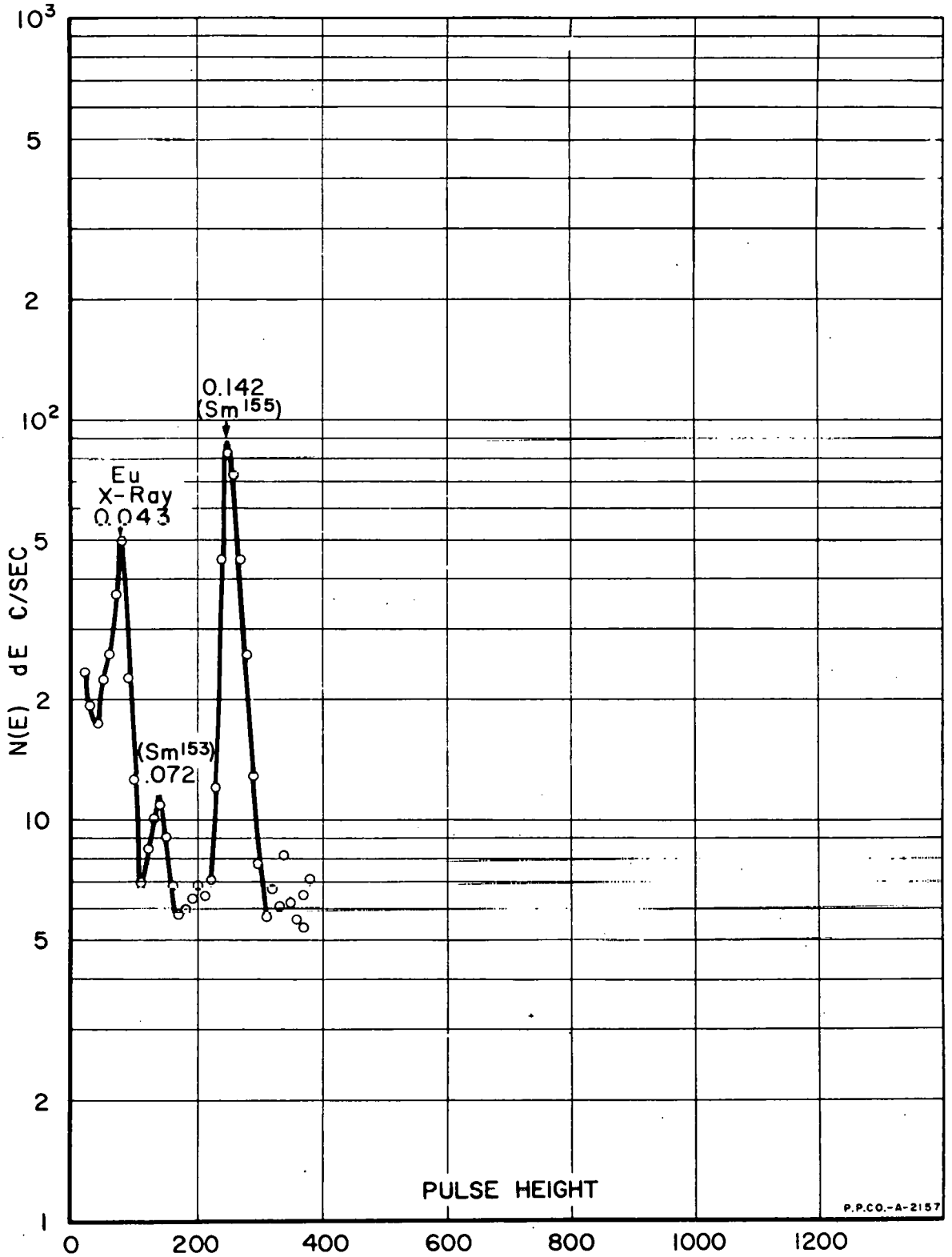

Fig. V-17 Coincidence gamma-ray spectrum showing radiation in coincidence with 0.106 Mev gamma-ray.

Table V-4

ENERGIES AND INTENSITIES OF Sm-155 GAMMA-RAYS

Gamma-Ray Energy, Mev	Relative Intensities
0.043 (Eu K X-ray)	0.25 ± 0.01
0.106 ± 0.005	1.00
0.142 ± 0.005	0.034 ± 0.003
0.245 ± 0.005	0.050 ± 0.005

e. Discussion

From the preliminary experimental evidence discussed, the major features of a level scheme for Eu-155 are proposed, as shown in Fig. V-18. Measurements are presently in progress to obtain information on the beta-ray energies and branching ratios.

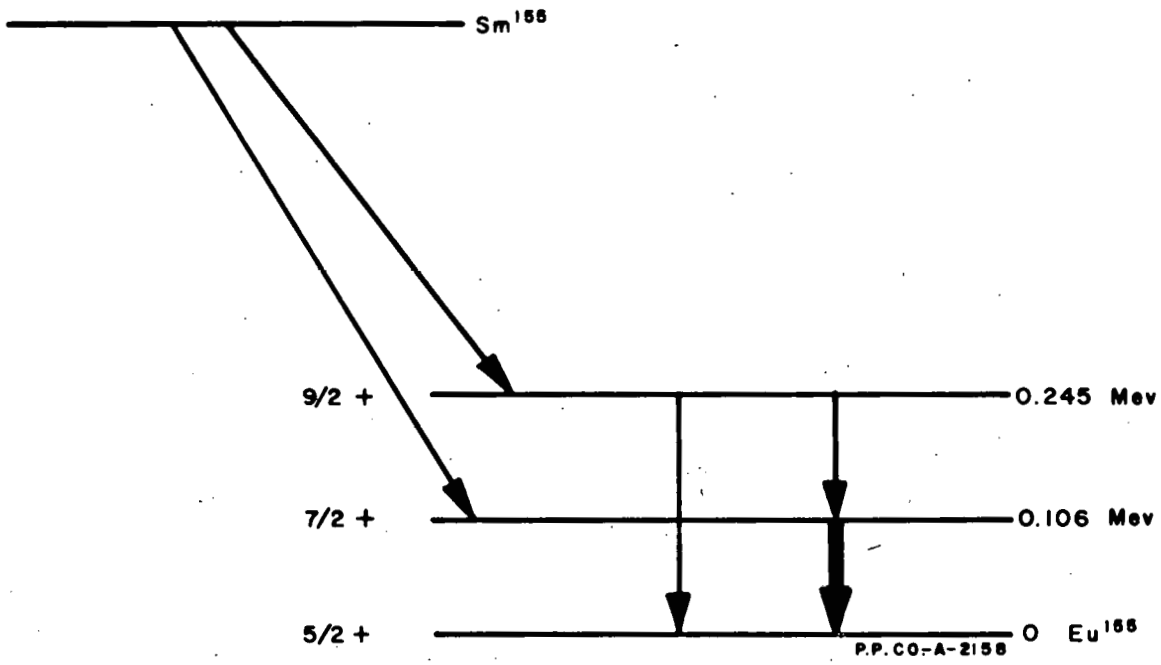

Fig. V-18 Proposed level scheme for decay of 23 minute Sm-155.

For highly deformed nuclei of odd A the unified model has been most successful in predicting the level structure. The low-lying states are generally found to exhibit a rotational spectrum with $I_o = K = \Omega$ $I = I_o$, $I_o + 1$, $I_o + 2$, ----, with all levels in a given band having the same parity. The energies of the levels of such rotational spectra are given by:

$$E = \hbar^2 \left[I(I + 1) - I_o + 1) \right] /2J$$

where I_o is the ground state spin.

If the ground state of E-155 is assumed to be 5/2 + (from the measured spins of near odd A nuclei, and decay data on Sm-153) the ratio of energies of a rotational spectrum for a spin sequence $9/2 + \rightarrow 7/2 + \rightarrow 5/2 +$ may be computed. From this is calculated a ratio of 2.28 for the first two levels. The experimental ratio of 0.245/0.106 = 2.31. From this it is concluded that the 0.245 Mev gamma would be E2 radiation and the 0.142 and 0.106 gammas would be characterized by a mixture of M1 and E2 radiation. Internal conversion coefficients and directional correlation measurements are presently in progress to substantiate these assignments.

2. Absolute Beta-Ray Counting Using a 4 π Windowless Flow Proportional Counter (E. C. Yates)

a. Introduction

In the determination of complete nuclear level schemes for radioactive nuclides it is necessary to know the total disintegration rate for radioactive sources with a high degree of precision. For beta emitters the most direct and accurate method of determining the disintegration rate is to count the individual particles emitted in a 4 π geometry, using gas-flow proportional counters. The major advantage of this method is that it is almost independent of the disintegration scheme. The only requirement is that one ionizing particle be emitted per disintegration.

Absolute beta-ray counting is a highly developed combination of many techniques. The most important effects which must be considered are absorption and scattering by the source support and self-absorption of the beta particles by the source material. To minimize these effects highly refined techniques for source preparation must be used. In the interest of applying these techniques in the determination of level schemes, a re-examination of the problems and previously employed solutions was necessary. Various types of gas-flow proportional counters and electronic systems were investigated together with techniques for source preparation. As a result of these studies a 4 π counting system has recently been placed into operation. Preliminary studies of operational characteristics indicate that reliable precision determination of absolute beta disintegration rates may be readily obtained.

b. Description of Counter and Electronics

The 4π proportional counter consists of two straight-wire, cylindrical, windowless ionization chambers. A sample slide is provided which is sealed by O-rings to permit fast insertion of samples with minimum atmospheric contamination of the counting gas. This feature facilitates the counting of short-lived activities by reducing the purging time.

The wide range of pulse sizes produced by a proportional chamber in the detection of beta particles requires the use of an electronic amplification system with almost ideal overload characteristics. Sufficient amplification to insure that the smallest pulses from events occuring in the chamber exceed the discriminator threshold implies that many pulses will be produced which are 100 to 1000 times the overload point at the amplifier output. The A-8 linear pulse amplifier, a double-differentiated amplifier recently developed by G. G. Kelley of ORNL,* exhibits improved characteristics for this application. This circuit also eliminates bias shifting and provides stable operation at high input counting rates with a dead time of 2 μsec.

To reduce the absorption of low energy beta particles in the source mounts, it is necessary to use thin film techniques. By use of the procedures developed by Pate and Jaffe,** suitable films have been obtained from a Bakelite plastic material, VYNS. This technique yields rugged films with a thickness of 6 $\mu g/cm^2$. To produce a region of non-zero field in the immediate vicinity of the source, a 2 $\mu g/cm^2$ conducting layer of gold is deposited by vacuum evaporation.

The counter system exhibits almost ideal operational characteristics. Fig. V-19 is a plot of the counting rate obtained from a Cs-137 source with sufficient gain in the system to drive all pulses originating in the counter to amplifier overload. This ideal pulse height distribution is an indication of the superior characteristics of the counter and electronic system, and the quality of the source. Fig. V-20 is a plot of counting rate vs counter voltage (so-called plateau curves) for Ni-63, Nb-95, Fe-59, and Cs-137, with beta end-point energies of 67, 160, 462, and 514 kev respectively. The plateau obtained for Ni-63 indicates a need for further refinement of source preparation techniques.

---

* G. G. Kelley, as reported in "Physics Division Semi-Annual Progress Report", 55, ORNL-2204 (1956).

** B. D. Pate and L. Jaffe, Can. J. Chem., 33, 15 (1955).

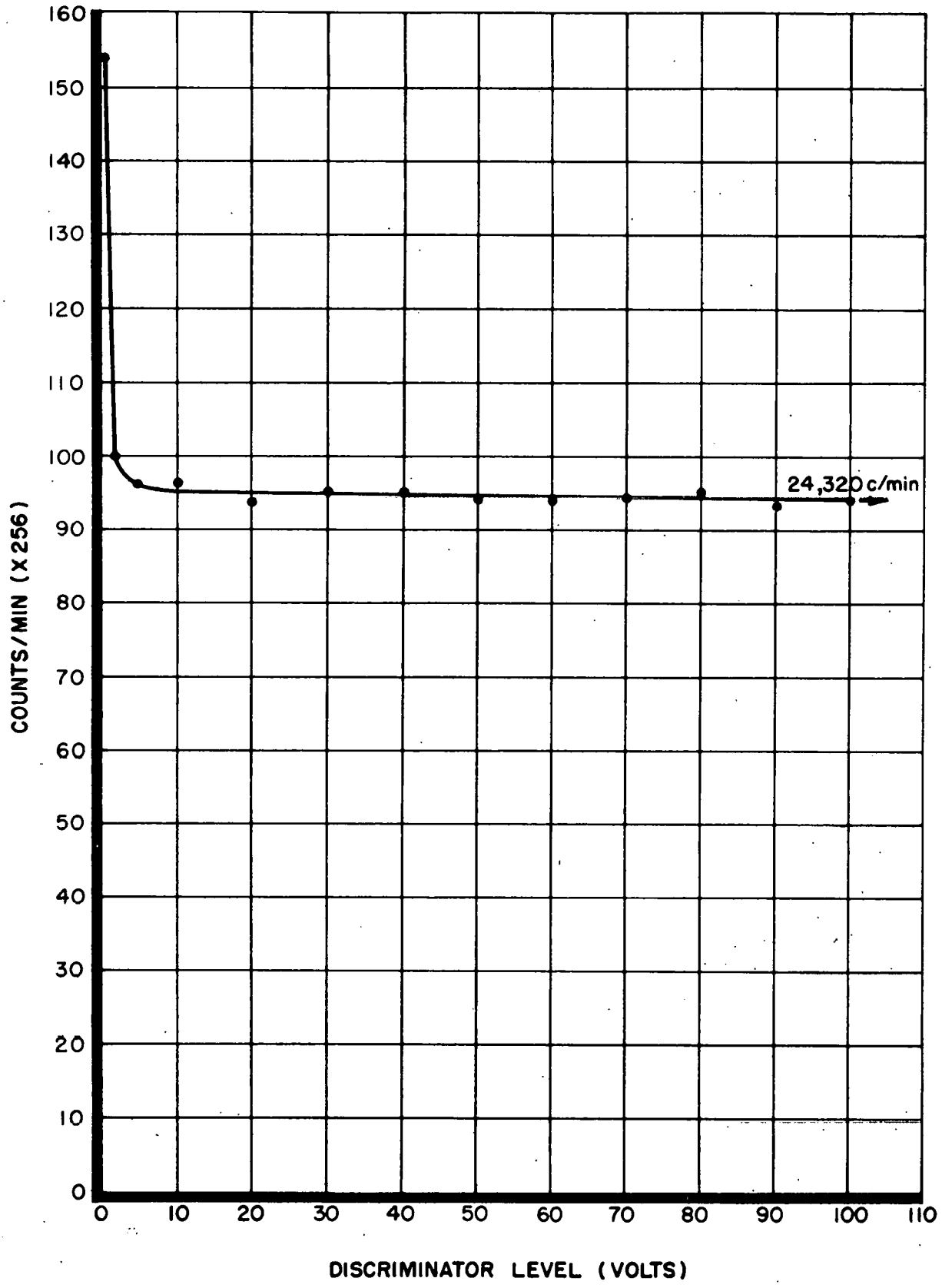

Fig. V-19 Proportional counter discrimination curve using A-8 amplifier (weak Cs-137 source).

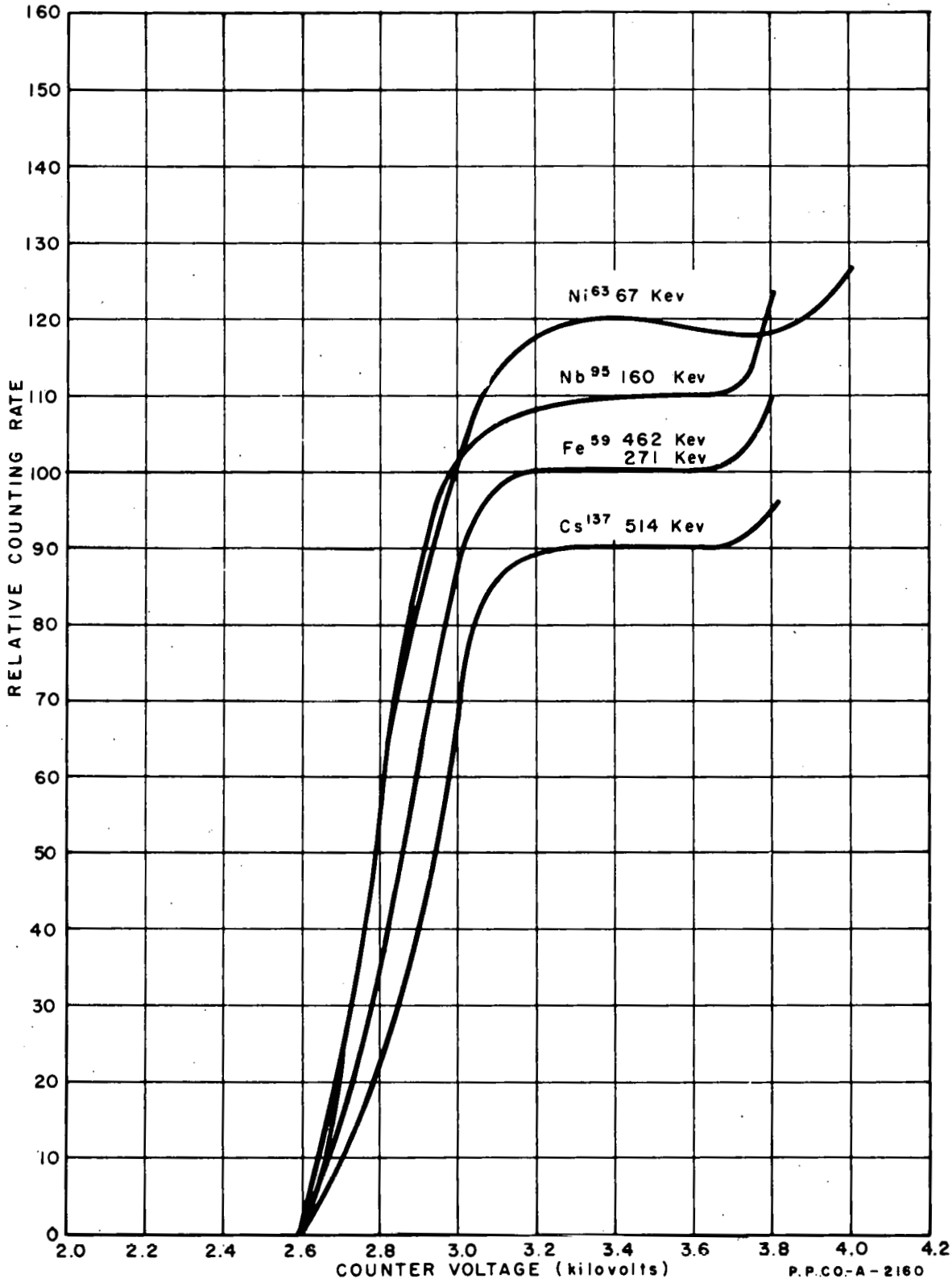

Fig. V-20 High voltage characteristics of 4 π proportional counter.

VI. THEORETICAL PHYSICS

A. A Two Dimensional Study of ETR Fluxes and Burnout with the IBM-704 Program "TURBO" (R. A. Grimesey and W. B. Lewis)

Flux variations occur in the ETR over the lifetime of the core, due to the cumulative effects of burnout and the shim rod withdrawal pattern. An attempt is being made to reduce them by choosing an optimum shim rod withdrawal pattern which will minimize distortion due to poison distribution and non-uniform burnout distribution. To study in detail the flux history of the ETR for a particular loading, the two-dimensional IBM-704 code "TURBO" was used. A rather complete flux history was obtained experimentally for Cycle 2 and it was decided to use "TURBO" to reproduce a similar flux history for Cycle 2, and at the same time obtain a more detailed space-time picture of ETR fluxes for use in attempting to choose an optimum shim rod withdrawal pattern.

The results of the initial study of fluxes and burnout for Cycle 2 indicate that TURBO is well adapted to the study of ETR flux histories. Full details of the procedure and results outlined here will appear in a topical report now being written.

TURBO, a two-dimensional burnout code based on diffusion theory, with its own library of cross sections, is described in detail elsewhere.* In this study, a modified program was used which is not yet included in WAPD-TM-95.* In the modified program the first ten compositions are made up of time-independent elements for which constant macroscopic cross sections are used. The elements of all other compositions are described by their atom densities, thermal self-shielding factors, and thermal cross sections; and their cross sections for the three fast groups are obtained from the TURBO library built into the code.

The TURBO study of the ETR consisted of ten separate time-steps where each time-step is the time required for withdrawal of a single shim fuel section. The time-dependent elements were depleted for each time-step by an amount appropriate to the power, length of time, and core configuration during this period. The composition for the shim rod which is moved during a time-step has the atom densities for a gray rod poison section replaced at the start of the time-step by those for a shim fuel section. The spatial calculation for this time-step is then performed based on the atom densities for the new shim fuel section, and the depleted atom densities arrived at during the previous time-steps for all other locations. At the end of the spatial calculation, the depletions in the time-dependent atom densities are computed assuming the fluxes and cross sections in each location remain constant during the time it took to pull this fuel section into the core. The data obtained for each time-step from the calculation consisted of the following in addition to the Supervisory-on-Line-Printout:

1. Pointwise power.
2. Pointwise macroscopic cross sections and constants for the four energy groups.

---

* J. B. Callaghan, et al., "TURBO--A Two-Dimensional Few-Group Depletion Code for the IBM-704", WAPD-TM-95 (1957).

3. Pointwise fluxes for each of four groups.

4. Flux-weighted average macroscopic cross sections and constants for each composition and each group.

5. Pointwise atom densities for boron and U-235.

6. Composition averaged atom densities.

All of the above data from TURBO were based on a core mockup consisting of 3125 mesh points and 23 compositions. A diagram of the core is shown in Fig. VI-1 and the initial 23 compositions are described in Table VI-1. The composition numbers for the gray rod poison sections are numbered consecutively in the order in which they are withdrawn during the cycle. The 3125 mesh points were obtained by evenly spacing 4 mesh lines through each horizontal dimension of a 3-in.-square area. For the initial time-step the elements in a region were completely homogenized over that region and a double P-1 heterogeneous cell study* was made to obtain flux depression factors for the fuel plates. These were incorporated as thermal self-shielding factors for the boron and U-235.

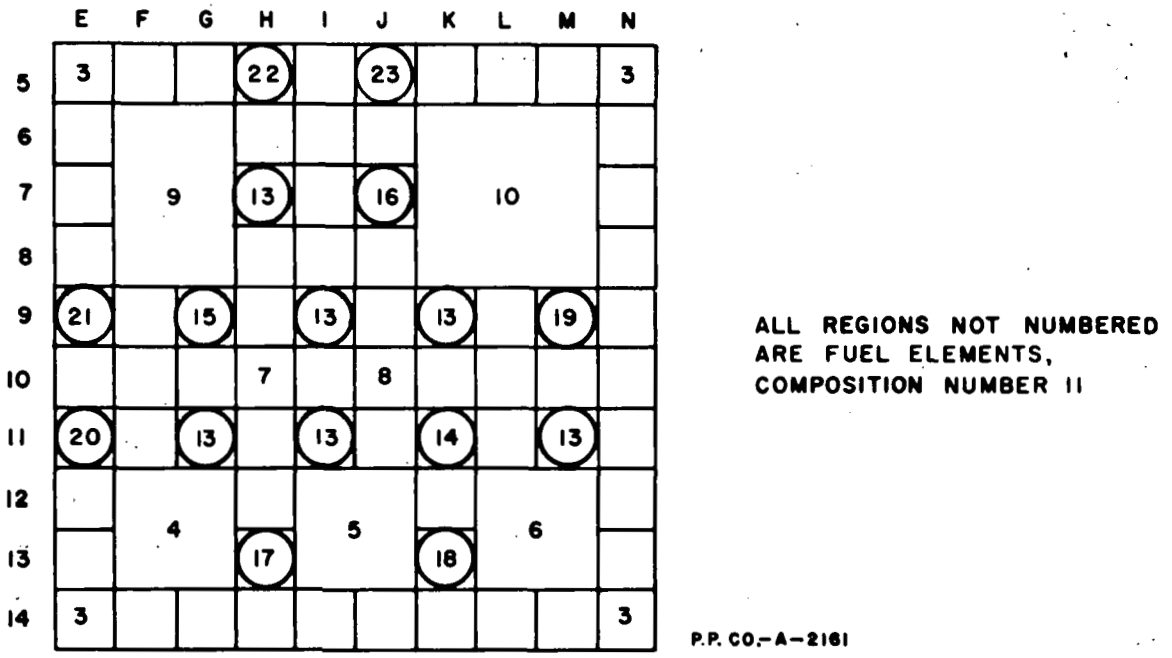

Fig. VI-1 Two-dimensional spatial composition description of the ETR core.

* E. Gelbard, "Iterative Solutions of the P_L and Double P_L Equations," WAPD-T-810 (1958).

Table VI-1

INITIAL DESCRIPTION OF THE 23 COMPOSITIONS

Composition No.	Composition Description	Atom Densities 10^{24} atoms/cc	
1	Aluminum Reflector	N_{Al}	0.0560
		N_{Water}	0.00234
2	Beryllium Reflector	N_{Al}	0.000467
		N_{Be}	0.1072
		N_{Water}	0.003358
3	Core Corner Filler Pieces	N_{Al}	0.0137
		N_{Water}	0.02557
4 - 10	Aluminum Filler Pieces in Core Experimental Holes	N_{Al}	0.04784
		N_{Water}	0.00683
11 - 12	Fuel Elements	N_{Al}	0.02343
		N_{Water}	0.0200
		N_{U-235}	0.0001207
		N_{B-10}	0.000002456
13 - 14	Shim Fuel Sections	N_{Al}	0.03252
		N_{Water}	0.01507
		N_{U-235}	0.0000534
		N_{B-10}	0.0000009924
15 - 23	Gray Rod Poison Sections	N_{Al}	0.01233
		N_{Water}	0.0186
		N_{Ni}	0.0204

In Fig. VI-2 (parts a-d) there is presented a history of the thermal flux for the center of each 3-in.-square section of the core. The fluxes for the reflectors and for some of the core positions are not presented because measured values are not available. The relative values of the fluxes are the only significant values because of the way in which an average power per unit height of core was assigned. With the exception of a few points, the time variation of the thermal flux agrees very well with the measured values. Table VI-2 gives the fraction of total power obtained from the fuel elements and shim fuel sections during the cycle that was studied.

Within the accuracy of the Cycle 2 flux measurements, the calculated fluxes from TURBO were in agreement, although the agreement was limited. The calculations gave flux shapes in much more detail than was possible in the measurements, and the general trends of the flux variations over the cycle were in good agreement. Thus it has been demonstrated that TURBO will be valuable for future ETR depletion studies. As a result of the TURBO depletion studies reported here, studies of the local flux perturbations due to ETR control rods are being initiated.

B. Calculations on the Scattering of Slow Neutrons by Free Water Molecules (G. W. Griffing)

A study of the scattering of slow neutrons by free water molecules, important to an understanding of neutron thermalization in water-moderated reactors, has been initiated here. Since the study is in the early stages, only preliminary considerations can be reported.

Goryunov* has considered the problem with a quantum mechanical approach. Upon comparing calculated values for the total cross section with experimental results for liquid water, he found the calculated values to be some 10% lower. It appears to be of interest to reconsider the work done by Goryunov since it is not clear whether the discrepancies** between the calculation and the experiments are due to certain approximations made in the computations, or to liquid binding effects.

---

* A. F. Goryunov, "Scattering of Slow Neutrons by Water Molecules", Soviet Journal of Atomic Energy 1, 3 (1956).

** T. J. Kreiger and M. S. Nelkin, "The Scattering of Slow Neutrons by Hydrogenous Moderators", KAPL-1597 (1956).

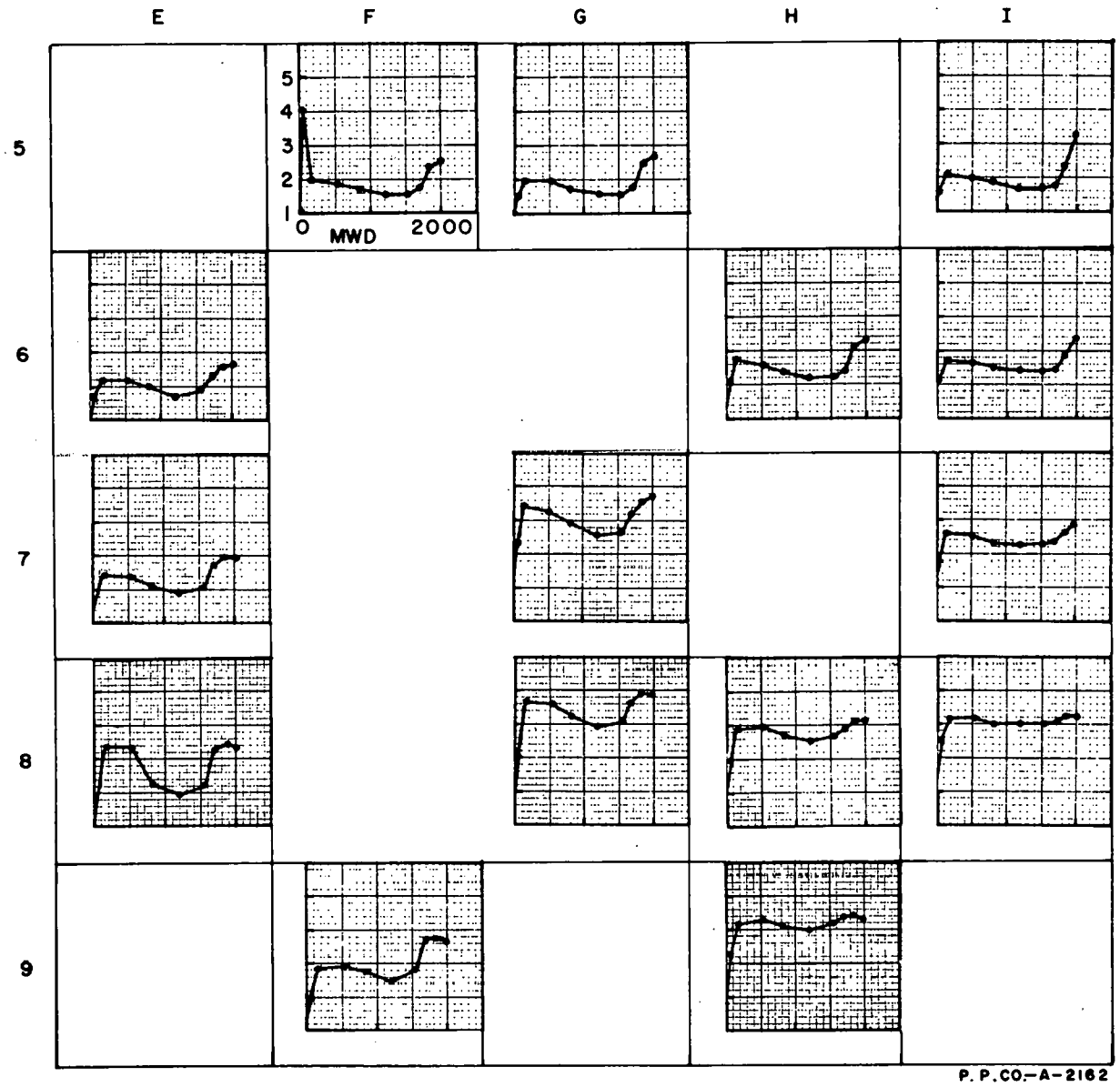

Fig. VI-2a Upper Left Quadrant - Thermal flux history at the center of each 3 in.-square section of the core.

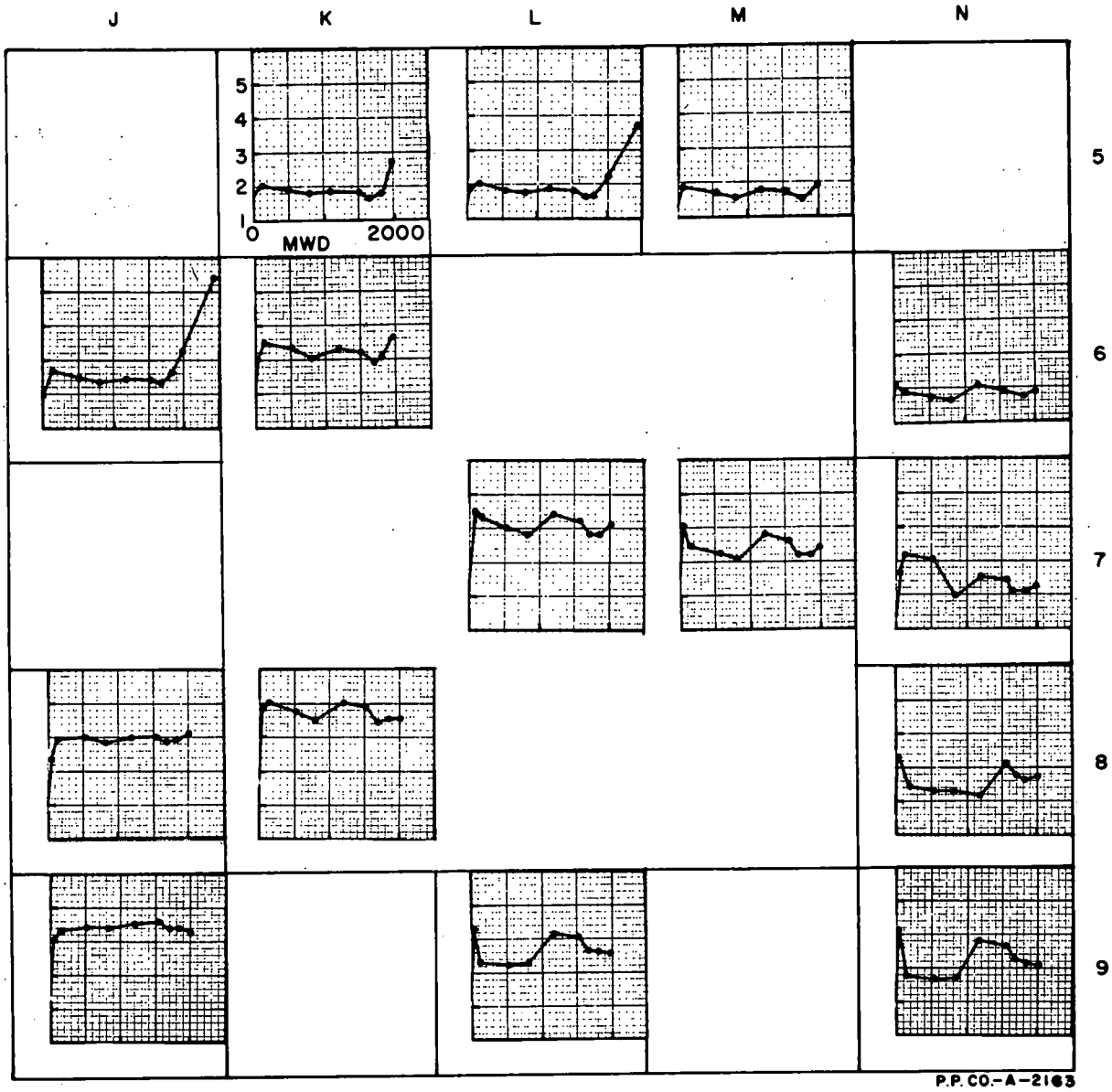

Fig. VI-2b Upper Right Quadrant - Thermal flux history at the center of each 3 in.-square section of the core.

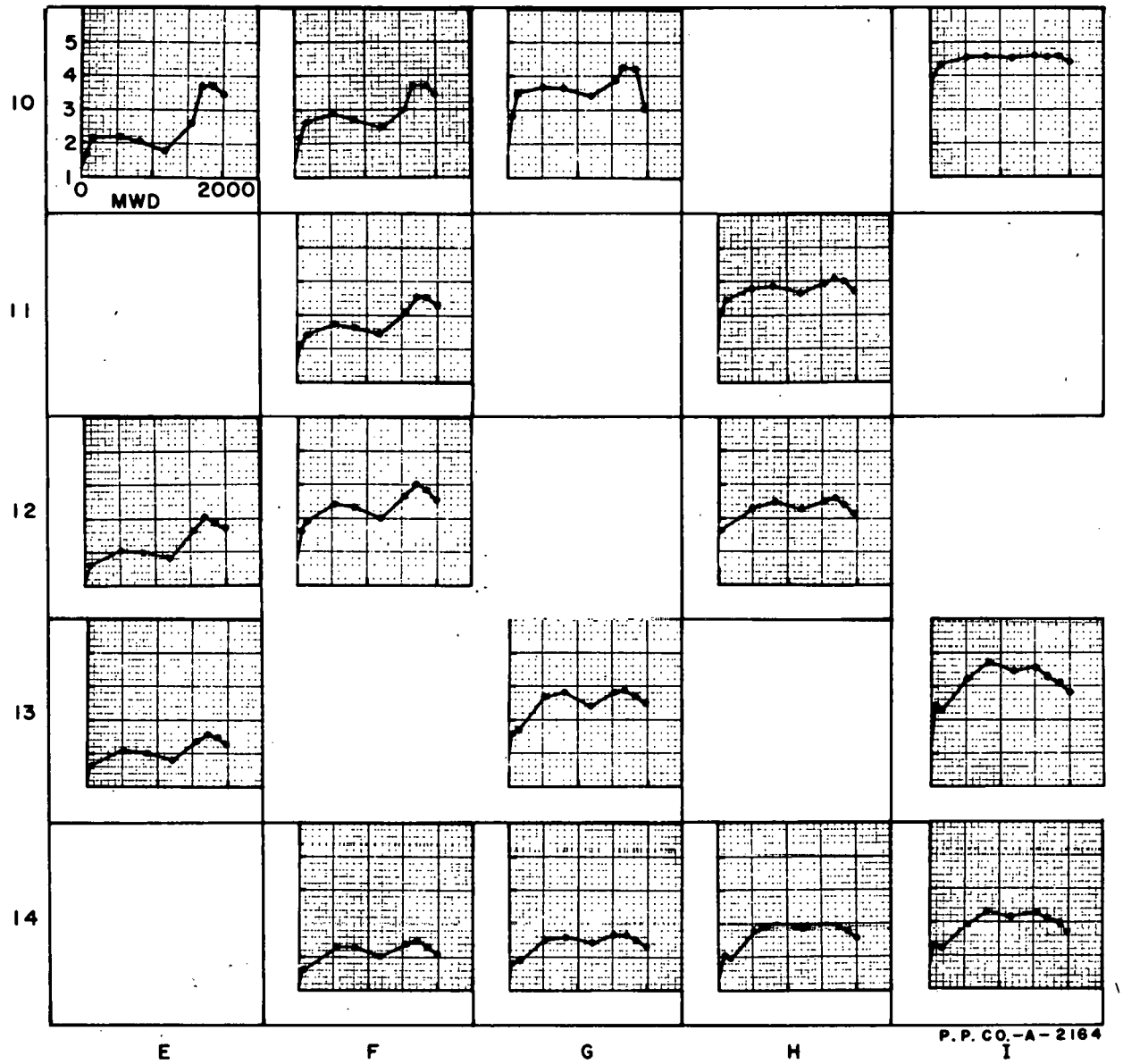

Fig. VI-2c Lower Left Quadrant - Thermal flux history at the center of each 3 in.-square section of the core.

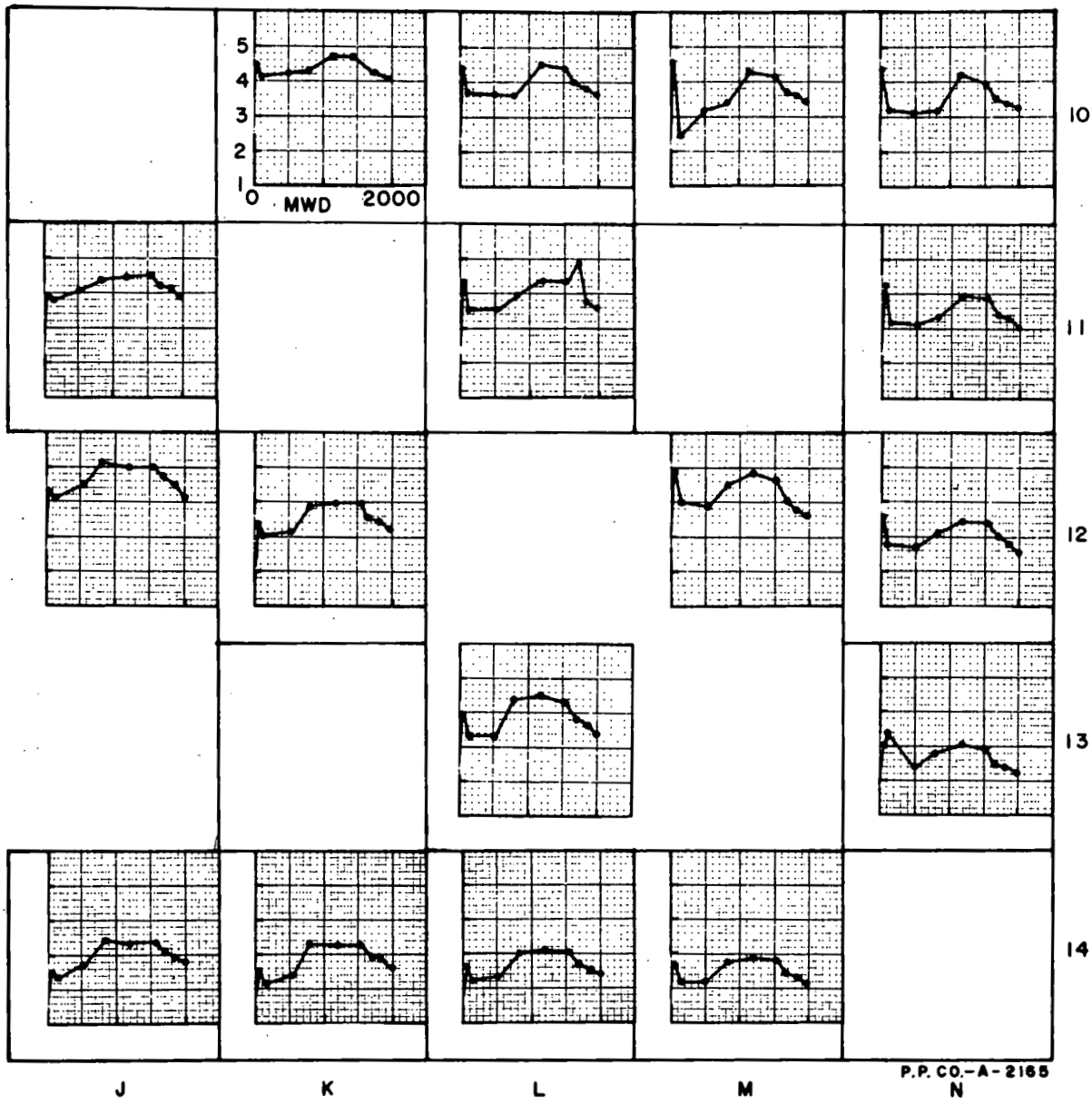

Fig. VI-2d Lower Right Quadrant - Thermal flux history at the center of each 3 in.-square section of the core.

Table VI-2

FRACTION OF TOTAL POWER GENERATED
IN EACH COMPOSITION FOR EACH TIME-STEP

Comp. Number	Time Step									
	00	01	02	03	04	05	06	07	08	09
11	.9022	.9003	.8809	.8754	.8700	.8656	.8593	.8451	.8397	.8342
12	.0188	.0173	.0212	.0203	.0179	.0155	.0171	.0237	.0248	.0241
13	.0664	.0648	.0654	.0639	.0618	.0598	.0581	.0560	.0547	.0531
14	.0126	.0123	.0108	.0106	.0112	.0111	.0104	.0094	.0088	.0084
15		.0533	.0109	.0105	.0096	.0086	.0089	.0099	.0099	.0095
16			.0107	.0098	.0090	.0089	.0084	.0080	.0082	.0900
17				.0094	.0096	.0086	.0088	.0086	.0080	.0074
18					.0109	.0102	.0097	.0086	.0080	.0075
19						.0116	.0105	.0092	.0088	.0086
20							.0086	.0104	.0099	.0093
21								.0111	.0109	.0103
22									.0081	.0094
23										.0093

The problem is being formulated in a manner similar to that used by Stig Brimberg* in work on the scattering of slow neutrons by hydrogen molecules. Work has been carried to the point where the wave functions for the water molecule, which is an asymmetric rotator, are needed in order to evaluate certain integrals occurring in the matrix elements for the cross section. What the best approach may be to this phase of the problem is not yet decided.

C. Applied Mathematics

1. Heat Conduction Equation (L. A. Schmittroth)

An IBM-650 program has been developed for two region temperature and heat flux calculations. The problem originated in SPERT's study of temperature and heat flux in a fuel plate during a transient. The heat equation is assumed in the form

$$\frac{\partial u}{\partial t} = f(u) \frac{\partial^2 u}{\partial x^2} + \frac{S(t)}{g(u)}$$

with $u(x,0) = h(x)$, $u_x(0,t) = 0$, and $u(b,t) = P(t)$. Below is a diagram of the situation.

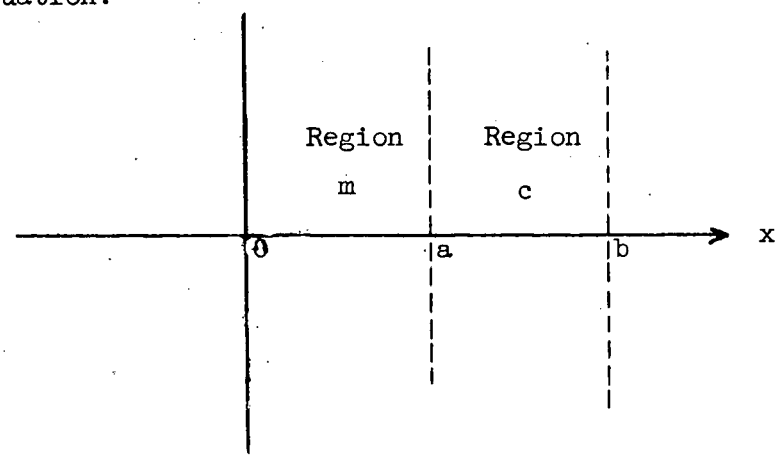

The coefficient $f(u)$ is assumed equal to $f^m(u)$ in region m and equal to $f^c(u)$ in region c. Similarly $g(u) = g^m(u)$ in m and $g^c(u)$ in c. The flux across $x = b$ is computed from $-K(u) \frac{u}{x}_{x=b}$, where $K(u)$ is a known function of temperature. The source S is assumed regionwise constant but time dependent.

The partial differential equation was replaced by a six-point finite difference approximation, and the resulting system of linear equations solved for each time-step. The program has been tested for constant coefficients against analytic solutions and has given excellent numerical accuracy.

---

* Stig Brimberg, "On the Scattering of Slow Neutrons by Hydrogen Molecules", Proceedings of the Second United Nations International Conference on the Peaceful Uses of Atomic Energy, Geneva 1958, 15, 79 (Paper 154).

The five functions $f^m(u)$, $f^c(u)$, $g^m(u)$, $g^c(u)$, and $K(u)$ must be programmed as subroutines in any particular application. The initial values $u(s,0)$ are read in at the start, and values of S^m, S^c, and P must be read in at each time-step.

The more general case

$$\frac{\partial}{\partial t}\left[c(u)\ u\right] = \frac{\partial}{x}\left[K(u)\ u\right] + S$$

with c and K assumed to be linear functions of u, and with more regions and more general boundary conditions, will be programmed by means of the same basic methods.

2. Fourier Analysis of Periodic Wave Forms (Anna Healy)

An IBM-650 program for Fourier Analysis of periodic wave forms has been written and checked out. The initial use of the program was by the Instrument Development Section to determine harmonic content of filtered wave forms. The program can handle up to 100 data points and 49 harmonics. The data points must be equi-spaced. The program computes by a least-squares fit to the data points the coefficients of $A_0 + A_1 \cos x + A_k \cos kx + B_1 \sin x + \ldots + B_k \sin kx$.

3. Numerical Inversion of Laplace Transforms (L. A. Schmittroth and R. Clayton)

The IBM-650 program for direct numerical inversion of Laplace Transforms has been checked out and is available for general use. The request for development of this method came from the Reactor Physics Branch. The program will be used to study the transient behavior of reactor control systems. Details may be found in a report soon to be issued.*

* L. A. Schmittroth and R. L. Clayton, "A Numerical Method for Computing Inverse Laplace Transforms", IDO-16525 (1959).

VII. PAPERS AND PUBLICATIONS

A. AEC Report Issued

IDO-16470, 1024 Channel Time-of-Flight Analyzer for MTR Fast Chopper - Operating Manual, by F. L. Petree.

B. Paper presented at the New York American Physical Society Meeting (January 28-31, 1959)

R. M. Brugger,* R. E. Schmunk, L. W. McClellan, and J. E. Evans, Slow Neutron Scattering from Methane and Steam.

C. Journal Publications

R. B. Regier, Radiometric Determination of Krypton-85, Analytical Chemistry 31, No. 1, 54-55 (January 1959).

R. M. Brugger, L. W. McClellan, G. B. Streetman, and J. E. Evans, Inelastic Scattering of Cold Neutrons from Several Hydrogenous Liquids, Nuclear Science and Engineering 5, No. 2, 99-104 (February 1959).

---

* Speaker


Phillips
66